

Global Biogeochemical Cycles[®]

RESEARCH ARTICLE

10.1029/2024GB008446

Key Points:

- Restored upland ecosystems absorb small amounts of methane but release more nitrous oxide, resulting in a net warming combined effect
- The radiative cooling from carbon storage in restored ecosystems outweighs the warming from the other greenhouse gases even after 100 years
- Letting ecosystems regenerate naturally provides a net cooling “climate opportunity benefit” across all biomes relative to agriculture

Supporting Information:

Supporting Information may be found in the online version of this article.

Correspondence to:

S. S. Cooley,
savannah.cooley@nasa.gov

Citation:

Cooley, S. S., Moore, E., Martinez, J., Fahlen, J., Maybach, E., Gollerkeri, M., et al. (2025). global “climate opportunity benefit” of forest regeneration: Meta-analysis shows warming from soil CH₄ and N₂O is small relative to agriculture. *Global Biogeochemical Cycles*, 39, e2024GB008446. <https://doi.org/10.1029/2024GB008446>

Received 28 NOV 2024

Accepted 22 AUG 2025

Author Contributions:

Conceptualization: Savannah S. Cooley, Duncan N. L. Menge

Data curation: Savannah S. Cooley, Elisabeth Moore, Jianna Martinez, Jocelyn Fahlen, Erin Maybach, Maya Gollerkeri, Anjali Rao Vasa

Formal analysis: Savannah S. Cooley

Methodology: Savannah S. Cooley, Sian Kou-Giesbrecht, Alexandra M. Huddell, Duncan N. L. Menge

Project administration: Savannah S. Cooley, Duncan N. L. Menge

Resources: Sian Kou-Giesbrecht, Alexandra M. Huddell, Duncan N. L. Menge





Supervision: Savannah S. Cooley

Validation: Savannah S. Cooley

Visualization: Savannah S. Cooley

Writing – original draft: Savannah S. Cooley, Linnea Norton

Global “Climate Opportunity Benefit” of Forest Regeneration: Meta-Analysis Shows Warming From Soil CH₄ and N₂O Is Small Relative to Agriculture

Savannah S. Cooley^{1,2} , Elisabeth Moore¹, Jianna Martinez¹, Jocelyn Fahlen¹, Erin Maybach³, Maya Gollerkeri¹, Anjali Rao Vasa¹, Sian Kou-Giesbrecht⁴ , Alexandra M. Huddell⁵, Linnea Norton¹ , Kerry Cawse-Nicholson⁶ , Ruth DeFries¹, Maria Uriarte¹, and Duncan N. L. Menge¹ 

¹Department of Ecology, Evolution and Environmental Biology, Columbia University, New York, NY, USA, ²Earth Science Division, NASA Ames Research Center, Bay Area Environmental Research Institute, Moffett Field, CA, USA,

³Department of Earth and Environmental Sciences, Columbia University, New York, NY, USA, ⁴School of Resource and Environmental Management, Simon Fraser University, Burnaby, BC, USA, ⁵Department of Department of Plant and Soil Sciences, University of Delaware, Newark, DE, USA, ⁶NASA Jet Propulsion Laboratory, California Institute of Technology, Pasadena, CA, USA

Abstract Global assessments of ecosystem regeneration as a climate mitigation strategy have traditionally focused on CO₂, despite the acknowledgment that methane (CH₄) and nitrous oxide (N₂O) are also important greenhouse gases (GHGs). We conducted a meta-analysis of studies that measured soil CH₄ and N₂O fluxes in unmanaged, regenerating forested and savanna ecosystems, with a focus on understanding biome-specific differences in these GHG fluxes compared to a counterfactual of agricultural land use. We expected most regenerating ecosystems to act as small CH₄ sinks and relatively larger N₂O sources, with a net warming combined CH₄-N₂O effect. Three of the five forested biomes we studied followed this pattern: subtropical/tropical forest, subtropical/tropical savanna and temperate conifer forest (0.60 ± 0.30 , 0.15 ± 0.06 , and 0.83 ± 0.24 Mg CO₂e ha⁻¹ yr⁻¹, respectively). Results suggest that even after 100 years of regeneration, the radiative cooling of the climate from CO₂ sequestration in aboveground biomass exceeds the radiative warming driven by the net CH₄-N₂O effect among all ecosystems on average globally. We also found that the “climate opportunity benefit” of ecosystem regeneration—the difference in the net CH₄-N₂O effects of agriculture versus regeneration—yields a net cooling effect for all biomes. However, because the CH₄-N₂O effect diminishes the cooling effect of ecosystem regeneration, our results underscore that it is unsound to use ecosystem regeneration as a justification for continuing fossil fuel emissions.

Plain Language Summary When we let farmland return to nature, it helps fight climate change by removing carbon dioxide from the air. But what about other greenhouse gases? Our research analyzed studies measuring two other important greenhouse gases—methane and nitrous oxide—as landscapes transform from farms or other disturbances back into forests and savannas. We made a few important discoveries. Even though restored forests and savannas often release enough of these gases to cause warming, they release less than farms. We also found that the carbon dioxide absorbed by growing trees outweighs the warming effects of methane and nitrous oxide release from forest and savanna soils. However, this “net cooling effect” of regeneration is much lower than expected if methane and nitrous oxide were not considered. This research is important because it gives us a more complete picture of how ecosystem restoration affects climate change. While bringing back forests and savannas can help cool the planet, our work underscores a crucial point: we can't use ecosystem restoration as an excuse to keep burning fossil fuels. The climate benefits of restoration, while real, don't offset the need to reduce emissions.

1. Introduction

Global estimates of the climate mitigation potential of terrestrial ecosystem regeneration are critical for achieving international climate agreements (Cook-Patton et al., 2020; Gilroy et al., 2014; Heinrich et al., 2023; IPCC, 2022). While many studies emphasize plant removal of carbon dioxide (CO₂) from the atmosphere (e.g., Cook-Patton et al., 2020; Robinson et al., 2024), the climatic impact of soil fluxes of methane (CH₄) and nitrous oxide (N₂O) during regeneration remains less explored. Although less abundant than CO₂ in the atmosphere, CH₄ and

Writing – review & editing: Savannah S. Cooley, Elisabeth Moore, Jianna Martinez, Jocelyn Fahlen, Erin Maybach, Sian Kou-Giesbrecht, Alexandra M. Huddell, Linnea Norton, Kerry Cawse-Nicholson, Ruth DeFries, Maria Uriarte, Duncan N. L. Menge

N_2O are 85 and 298 times more potent per molecule than CO_2 over a 20-year timeframe (IPCC, 2022) and they account for 16% and 6% of overall radiative forcing, respectively (IPCC, 2021; Myhre et al., 2013). Including CH_4 and N_2O emissions can substantially modify global greenhouse gas budgets (Tian et al., 2015). Therefore, changes in the fluxes of CH_4 and N_2O during forest regeneration—as a consequence of the abandonment of agriculture or during succession following a major disturbance event—could offset or amplify the CO_2 storage benefits of ecosystem regeneration. Simultaneously, accounting for CH_4 and N_2O from agriculture is needed to comprehensively assess the climate implications of forest regeneration that replaces agriculture (Hayek et al., 2020; Huddell et al., 2020; Saunois et al., 2020; Tian et al., 2023).

Both the magnitude and sign of soil fluxes of CH_4 and N_2O vary substantially across ecosystems and environmental conditions. Most unmanaged forested and savanna ecosystems act as small but positive CH_4 sinks, absorbing more CH_4 through methanotrophy than they emit through methanogenesis, creating a net climate cooling effect (Hatano et al., 2016; Itoh et al., 2012; Nagano et al., 2012; Sinha et al., 2007; Zhao et al., 2019). However, inundated wetlands frequently act as net CH_4 sources because anoxia favors methanogenesis (Tian et al., 2015; Yavitt et al., 1990). Conversely, soils in unmanaged forested and savanna ecosystems typically emit more N_2O than they absorb, through a combination of nitrification and denitrification, creating a net climate warming effect globally (McDaniel et al., 2019; Tian et al., 2015). Under particularly wet conditions, however, N_2O can be consumed at higher rates than it is emitted, leading to a net sink in some regions (Tian et al., 2020).

To date, global international climate mitigation estimates of ecosystem regeneration do not consider CH_4 and N_2O soil fluxes (IPCC, 2022) due to limited knowledge about how these fluxes vary across large spatiotemporal scales and due to recognition that these fluxes have a smaller total radiative forcing impact relative to CO_2 (Hatano et al., 2016; Itoh et al., 2012; Melack & Hess, 2023; Tian et al., 2015). Most existing global meta-analyses of unmanaged ecosystems focus on either CH_4 (Dutaur & Verchot, 2007; Yvon-Durocher et al., 2014) or N_2O (Aronson & Allison, 2012; Borchard et al., 2019; Kim et al., 2013; Wang, Hu, et al., 2022; Zhang et al., 2022; Zheng et al., 2020; Zhou et al., 2022). Among those that incorporate both greenhouse gas (GHG) fluxes together, we found three studies that investigated how CH_4 and N_2O change through successional time (Feng et al., 2022; He et al., 2024; McDaniel et al., 2019). Studies have reported initial spikes in CH_4 and N_2O after conversion from mature forest to agricultural land use (cropland, pasture or tree plantation) followed by declines toward zero during the first several years after the land use change (Feng et al., 2022; McDaniel et al., 2019). However, the studies did not point to conclusive results for the longer timescales of unmanaged regeneration (defined by Feng et al. (2022), He et al. (2024) and McDaniel et al. (2019) over an 80-, 120- and 150-year period since previous land use, respectively). While Feng et al. (2022) found declines in both CH_4 and N_2O forest soil emissions during the first ~5 years of succession, McDaniel et al. (2019) found no significant effects through the 150 years of succession they examined. He et al. (2024) found significant declines in CH_4 soil emissions during ecosystem restoration, but this study combined data from grasslands and forests into the same model. He et al. (2024) did not find significant changes in N_2O soil fluxes for non-wetland ecosystems through restoration. This difference in results may be due to a lack of data and/or a lack of spatially explicit models. In other words, it remains unresolved whether soil fluxes of CH_4 and N_2O in unmanaged ecosystems change among biomes and through time since the last major disturbance or agricultural land abandonment.

Here, we built on these past studies to investigate CH_4 and N_2O fluxes during ecosystem regeneration. We conducted a new global meta-analysis to address three overall questions. (Q1) How do the net radiative effects of CH_4 and N_2O vary across natural forested and savanna biomes and through succession? (Q2) How does incorporation of the net radiative effects of CH_4 and N_2O modify the aboveground CO_2 sequestration benefits of forested and savanna ecosystem regeneration? (Q3) How do the net radiative effects of CH_4 and N_2O in natural forested and savanna ecosystems compare to those in agricultural ecosystems? Existing research points to some hypotheses for our questions. For example, for Q1, there is considerable variation in the sign and magnitude of CH_4 and N_2O fluxes among ecosystems globally (Kim et al., 2013). Therefore, we hypothesized wide variation in both CH_4 and N_2O fluxes across the biomes we studied: boreal forest, subtropical/tropical forest, subtropical/tropical savanna, temperate broadleaf forest and temperate conifer forest. We expected that most ecosystems would be CH_4 sinks but N_2O sources overall, and that the N_2O effect would outweigh the CH_4 effect (i.e., there would be a net warming effect). Additionally, given that soil moisture tends to decrease through succession (Guariguata & Ostertag, 2001; Hogan et al., 2022; Vasconcelos et al., 2004; though see Fest et al., 2015), we hypothesized an increasing CH_4 sink with increasing time since disturbance. As initial post-disturbance pulses of high N availability from mineralization decrease with plant uptake and growth, we expected N_2O emissions to

show a modest decreasing trend over successional time—modest relative to the interannual variability in N_2O emissions observed within biomes (Brümmer et al., 2008; Butterbach-bahl & Papen, 2002). For Q2, we hypothesized that accounting for the effects of CH_4 and N_2O would decrease the aboveground CO_2 sequestration benefit of ecosystem regeneration, but that regeneration would still be a net benefit. N_2O emissions from unmanaged ecosystems are usually lower than those from agriculturally managed systems enriched with synthetic and organic fertilizers (Brümmer et al., 2008; Huddell et al., 2020; Li et al., 2023), and CH_4 emissions from animal agriculture can be large (Saunio et al., 2020). Therefore, for Q3, we hypothesized that natural ecosystems would have a weaker net warming N_2O effect relative to agriculture and a small net cooling CH_4 effect similar in magnitude to the positive CH_4 fluxes (i.e., net warming) from agriculture.

2. Methods

2.1. Data Preparation

We obtained 12,003 peer-reviewed papers from the Web of Science database combining the following three search terms:

1. Nitrous oxide OR N_2O OR Methane OR CH_4 ; AND
2. forest* OR ecosystem* OR wood* OR jungle OR temperate forest OR mixed forest OR tropical forest OR subtropical forest OR rainforest OR moist forest OR wet forest OR dry forest OR arctic OR boreal OR tundra OR high latitude OR taiga OR subarctic OR grassland OR savanna OR desert OR shrubland OR dryland OR steppe OR meadow OR Cerrado OR Mediterranean OR fynbos OR chaparral OR matorral OR maquis OR kwongan OR tree OR shrub OR scrub OR herb OR *lichen OR cyanobacteria OR moss OR liverwort OR free-living OR heterotroph* OR soil crust OR biological soil crust OR biocrust OR cryptogamic crust OR *symbio* OR cyanolichen OR endophyt*); AND
3. age OR time OR succession OR regeneration OR regrowth OR disturbance OR degradation OR land use OR chrono* OR year*.

Of the original set of peer-reviewed papers returned in our search, we extracted data from 115 papers that met five criteria (Table S1 in Supporting Information S1). These criteria excluded studies focused on peatlands and fully inundated ecosystems (the latter defined as ecosystems where the water table was greater than or equal to 0 cm relative to the soil surface for over a month of the study duration period). The criteria also focused on studies that reported quantitative soil flux measurements and took place in forested and savanna biomes. If studies focused on measuring GHG fluxes in response to a treatment, then we used GHG measurements from the control plots only. For example, if a study included plots with different fertilizer treatments to test the effects of fertilization on GHG emissions, then we would only include the control plots that did not receive any fertilization treatment.

The measurement strategy employed by the studies in our analysis fell within three categories: chronosequence studies, “measurements through time” studies, or studies that featured both approaches combined. A chronosequence is a series of ecological sites that vary in age but share similar environmental conditions and soil types. Our inclusion criteria for chronosequence studies with a measurement period less than 2 years ensured that such studies included at least two plots of ages that differed more than 2 years. Studies that used a “measurements through time” approach consisted of GHG measurements of one or more plots of the same age. All “measurement through time” studies were required to have a measurement period greater than 2 years. Some studies measured chronosequence plots with a measurement period greater than 2 years. We considered these studies to form a third category of measurement by employing both approaches.

The final group of studies covered a range of geographical areas but were predominantly concentrated in Europe, North America, and Asia (Figure 1). Sample size varied among biome types (Figure S1 in Supporting Information S1). Temperate broadleaf forests had the largest sample size, with 414 plot-year observations (55.4%), whereas tropical savanna/grassland had the smallest sample size of 26 (3.5%). We collected data for previous land use or disturbance history corresponding to each study (Table S2 in Supporting Information S1). Previous land use and disturbance histories varied among observations. Mature ecosystems (free of any major disturbance for >200 years) comprised the largest subset of the observations ($n = 263$ or 35.2% of the total). Clear-cut forest comprised the second largest category ($n = 236$ or 31.5%) followed by agriculture abandonment ($n = 150$ total or 22.06% among all cropland, pasture and unspecified agricultural uses combined). Note that some of the plot-year observations reported here include measurements for both CH_4 and N_2O while others only include measurements

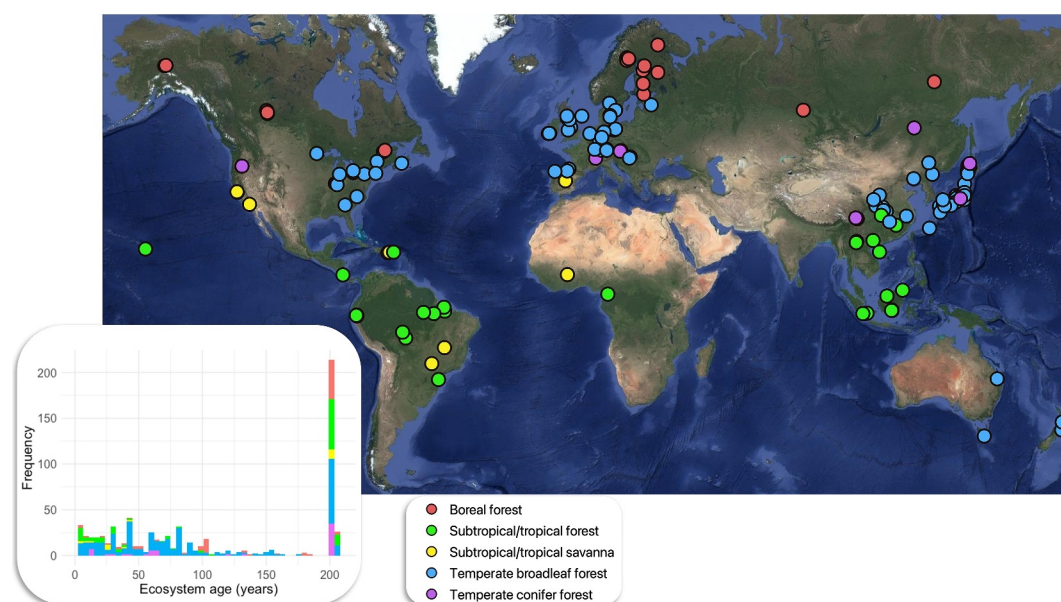


Figure 1. Locations of the measurement plots from the 115 studies in the meta-analysis colored by biome type. Inset: Histogram of ecosystem ages in the final data set.

for one but not the other GHG type. See Table S2 in Supporting Information S1 for the land use-specific breakdown of plot-year observations and Table S3 in Supporting Information S1 for the GHG-specific observation counts.

Among the total sample size of plot-year observations, 127 (17.0%) came from chronosequence studies, 346 (46.3%) came from measurements through time (minimum of 2 years between first and last measurement), and the remaining 275 (36.8%) employed both approaches combined. Among the studies that took measurements through time, the mean measurement period durations were 3.05 and 3.24 years for CH_4 and N_2O , respectively.

We recorded the age of the ecosystem reported in the original study. Numerous studies tracked changes in soil greenhouse gas emissions of old-growth forests whose ages were not reported. In these cases, we assumed ages to be 200 years. Our selection of the 200-year duration corresponds to the approximate maximum time frame we would expect sites to show evidence of a large-scale disturbance (Chazdon, 2003). This assumption allowed us to include these studies in our subsequent quantitative analyses. For consistency, we also set studies reporting ecosystem ages greater than 200–200 years at the start date of the data collection period. Ecosystem ages exhibited a bimodal distribution, with the second peak near 200 years due to the age binning of old-growth forests (Figure 1). The median and mean ecosystem age in the data corresponded to 63 and 94.1 years, respectively, with a standard deviation of 77.1 years.

When reported in the original study, we used fluxes that were already scaled to yearly estimates. If a study only provided flux estimates in a sub-yearly time scale, we averaged the available fluxes within each year and scaled them to annual rates as follows. For temperate and tropical studies, where sampling across the entire year was common, we assumed that the average of the measurements reflected the average annual rate and applied that rate to the year (e.g., if a study reported hourly GHG fluxes, we multiplied the hourly rates by $24 \text{ hr day}^{-1} \times 365 \text{ days yr}^{-1}$). In contrast, most studies of boreal forests collected measurements during the peak growing season. Thus, scaling fluxes by a constant in boreal regions would misrepresent the near-zero GHG fluxes during winter months. We applied a sampling bias correction to all Boreal forest observations to reflect that most observations were collected during summer months, when high temperatures drive soil thawing that leads to high soil moisture conditions and the potential for high microbial activity (Mason et al., 2019; Sinha et al., 2007). We adjusted for this by dividing the scaled yearly flux by 2 to follow the approximate length of the growing season (Sinha et al., 2007).

2.2. Statistical Analysis

The goals of our statistical analyses were to characterize how CH₄ and N₂O fluxes changed across space and through time (Q1), assess how the incorporation of the net radiative effects of CH₄ and N₂O offset the CO₂ sequestration benefits of forested and savanna ecosystem regeneration (Q2), and compare the net radiative effects of CH₄ and N₂O in natural forested and savanna ecosystems with those in agricultural ecosystems (Q3).

There was high variability in the CH₄ and N₂O fluxes (Figures S2, S3 in Supporting Information S1). To determine whether environmental variables driving greenhouse gas fluxes differed by biome, we first ran random forest regression analyses (compare Figure S4 with Figure S5 in Supporting Information S1). These analyses confirmed that the importance of different environmental variables in predicting CH₄ and N₂O fluxes varied substantially by biome. Based on this finding, we decided to model each biome separately.

Since GHG fluxes were highly skewed, we fitted biome-specific mixed-effect gamma regression models explaining CH₄ and N₂O fluxes for boreal forest, subtropical/tropical forest, subtropical/tropical savanna, temperate broadleaf forest and temperate conifer forest. We used the Annual International Geosphere-Biosphere Programme (IGBP) classification system land cover map to delineate the distributions of each biome. We treated the study as a random effect (i.e., each study had a unique intercept) to control for differences in methodologies and site characteristics across studies. The biome-specific models used a gamma log link function.

To obtain positive values necessary for gamma regression, we transformed CH₄ and N₂O observations by adding the absolute value of the minimum of all the GHG (CH₄ or N₂O) flux observations plus 1.0001 to each soil flux observation: $\text{GHG flux}_{\text{scaled}} = \text{GHG flux}_{\text{original}} + |\min(\text{GHG fluxes})| + 1.001$, where GHG flux is the CH₄ or N₂O soil flux observation and GHG fluxes is the corresponding set of all soil flux observations in the data. To simplify running the models and interpreting results, we standardized all covariates by subtracting the mean from each observation and dividing this by the standard deviation.

For each biome-specific model, we used a model selection approach based on Akaike's Information Criterion (AIC) to determine the optimal number of covariates. We started with a base model (m1) that included only ecosystem age and then systematically added covariates in order of their importance as determined by random forest variable importance measures (Figure S5 in Supporting Information S1). For each biome and greenhouse gas combination, we evaluated models of increasing complexity (m1–m3), where each subsequent model added one additional covariate. The final model for each biome-greenhouse gas combination was selected based on the lowest AIC value, resulting in varying numbers of covariates across the different models (Table S3 in Supporting Information S1). This approach optimized model performance while avoiding overfitting.

We tested all models for heteroscedasticity using the Breusch-Pagan test and for normality of residuals using the Shapiro-Wilk test (Table S4 in Supporting Information S1). In cases where heteroscedasticity was detected ($p < 0.05$ in the Breusch-Pagan test), we implemented robust mixed-effect models using the `robustlmm` R package, which applies techniques that are less sensitive to heteroscedasticity and outliers. This approach resulted in similar intercept and coefficient values from the originals (see comparison in Table S4 in Supporting Information S1). We therefore decided that the small change in coefficient values we observed did not justify the added complexity of using the robust modeling approach, so we used the original tests for our main results.

We also conducted a sensitivity analysis to evaluate model stability across different modeling choices, including outlier removal strategies and random effects structures (Table S5 in Supporting Information S1). For each gas-biome combination, we tested sensitivity to: (a) outlier removal (none vs. removal of observations beyond ± 3.5 SD), and (b) random effects structure (random intercept vs. random slope). This analysis quantified the variability in Age coefficient estimates and identified which findings were most robust.

The covariates we assessed consisted of 18 climate variables including precipitation seasonality, mean annual precipitation, temperature seasonality and mean annual temperature from the WorldClim bioclimatic variables (Fick & Hijmans, 2017) as well as topographic variables including elevation, slope and aspect from the USGS Global Multi-resolution Terrain Elevation Data (Danielson & Gesch, 2011) and soil composition variables including soil texture, soil porosity, % sand, % silt and % clay from the World Soil Database version 1.2 (UN FAO, 2012). We recognize that soil moisture is an important driver in the production and consumption of both CH₄ (Teixeira et al., 2020; Vasconcelos et al., 2004; Verchot et al., 2000; Wang, Gao, et al., 2022) and N₂O (Itoh et al., 2012; Kim et al., 2013). However, soil moisture data were not provided for some of the studies in our meta-

analysis and the spatial resolution of existing global satellite-based soil moisture products was too coarse to be useful (~9 km per pixel).

To address Q1, we included Age as a covariate in all biome-specific models. The remaining covariates were selected based on the output of variable importance measures from random forest regression computed for each biome (Figures S5, S6 in Supporting Information S1) in the same way the uncorrelated best-performing covariates for the global model were selected. If correlations between the top-ranking variables exceeded 0.35, then the next best performing variable was used.

Each biome-specific model took the following general form:

$$\text{CH}_4 \text{ flux}_{\text{scaled}} \sim B_0 + \delta_i + B_1 * \text{Age} + [B_2 * \text{Var2}] + [B_3 * \text{Var3}] + [B_4 * \text{Var4}] + \varepsilon \quad (1)$$

$$\text{N}_2\text{O flux}_{\text{scaled}} \sim B_0 + \delta_i + B_1 * \text{Age} + [B_2 * \text{Var2}] + [B_3 * \text{Var3}] + [B_4 * \text{Var4}] + \varepsilon \quad (2)$$

where $\text{CH}_4 \text{ flux}_{\text{scaled}}$ and $\text{N}_2\text{O flux}_{\text{scaled}}$ are the positively scaled CH_4 and N_2O soil fluxes extracted from the studies included in our meta-analysis, where positive scaling consisted of adding the absolute value of the minimum soil flux to each observation plus 1.0001 as described above; B_0 is the fixed-effect intercept; δ_i is the random variation in the intercept for each study i ; B_1 is the coefficient of Age, the age of the ecosystem (originally in years but unitless because of the standardization $\text{Age} = (\text{Age}_{\text{original}} - \text{mean}(\text{Age}_{\text{original}}))/\text{sd}(\text{Age}_{\text{original}})$); B_2 , B_3 and B_4 are the coefficients of the standardized (as described for Age) best-performing, uncorrelated fixed-effect variables identified based on a random forest variable importance measure of % increase in mean squared error computed for each biome-specific model. The number of included variables varies by biome and gas combination depending on the optimal model selected through AIC comparison. Terms in square brackets ($[B_2 * \text{Var3}]$, $[B_3 * \text{Var3}]$ and $[B_4 * \text{Var4}]$) may be excluded in some models if their inclusion did not improve model performance; and ε is residual error.

To compare the effects of CH_4 and N_2O to each other and to CO_2 , we defined the “net CH_4 - N_2O effect” to be the sum of the radiative forcing from CH_4 (modeled in Equation 1) and N_2O (modeled in Equation 2) in CO_2 -equivalents. We reported the net CH_4 - N_2O effect as CO_2 -equivalent fluxes to account for the radiative differences in N_2O and CH_4 in the atmosphere: over a 20-year horizon, CH_4 is 85 times as potent of a greenhouse gas as CO_2 while N_2O is 298 times as potent of a greenhouse gas as CO_2 (IPCC, 2022). A positive CH_4 - N_2O effect indicates a net warming effect on the climate, whereas a negative CH_4 - N_2O effect indicates a net cooling effect. We also computed the same models using a 100-year time horizon for the global warming potential (Table S6 in Supporting Information S1). We focused on the 20-year horizon for the main results for two main reasons. First, a 20-year horizon provides a more conservative estimate (stronger CH_4 effect and relatively smaller change in the N_2O effect). Second, a 20-year horizon is increasingly being adopted by the climate science community to improve climate science communication, highlighting the immediacy and urgency of the climate crisis (Abernethy & Jackson, 2022).

The global net CH_4 - N_2O effect was calculated by upscaling the spatially explicit model predictions. First, the net CH_4 - N_2O effect predictions from the best-performing biome-specific models were rasterized onto a global grid with a 0.5-degree resolution. The area of each grid cell was calculated in hectares, and this area was multiplied by the corresponding predicted net GHG flux (in $\text{Mg CO}_2\text{e ha}^{-1} \text{ yr}^{-1}$) to determine the total flux for each pixel. Finally, the total global net effect was computed by summing the flux values of all non-NA grid cells across the globe.

Unlike other global meta-analyses of N_2O and CH_4 (Feng et al., 2022; He et al., 2024; McDaniel et al., 2019), we did not use a statistical approach that would require the pairing of control-treatment plots (where “treatment” is defined as the disturbed or regenerating plot and “control” as the mature/old-growth forest plot). Requiring this pairing would have eliminated many of the measurement through time studies from our analysis and therefore limit the sample size and strength of our results.

2.3. Net Radiative Effects of CH_4 and N_2O Relative to Aboveground CO_2 Sequestration Through Time

Using the results of the statistical analyses described in Equations 1 and 2 above, we modeled the net radiative effects of CH_4 and N_2O through regeneration time with a 100-year timeframe. We chose to use a 100-year time

period for regeneration to be consistent with previous work (Feng et al., 2022; McDaniel et al., 2019; Robinson et al., 2024), though we acknowledge that many forests do not regenerate for this long due to anthropogenic as well as climate-induced disturbances including agriculture, logging and fire (Schwartz et al., 2020). Each biome-specific model took the following general form:

$$\text{Net CH}_4\text{--N}_2\text{O effect} = \int_0^{100} B_{0_br} + B_{1_br}t \, dt \quad (3)$$

$$= B_{0_br} * t + \frac{B_{1_br} * t^2}{2} \Big|_0^{100} \quad (4)$$

where net CH₄–N₂O is the joint radiative effect of CH₄ and N₂O soil fluxes; t is the age of the ecosystem in years; B_{0_br} is the sum of the back-transformed CH₄ and N₂O fixed-effect intercepts of the statistical models described in Equations 1 and 2, respectively (back-transformed to original unscaled units of Mg CO₂e ha^{−1} yr^{−1}); and B_{1_br} is the sum of the back-transformed CH₄ and N₂O coefficients of Age, the age of the ecosystem (back-transformed from standardization to original units of years). Note that for extending results over 100 years, we treated the other variables in Equations 1 and 2 as though they were also equal to their mean values (i.e., the variables were assumed to equal 0 because of biome-specific standardization).

To address Q2, we determined an adjusted climate mitigation impact of ecosystem regeneration through time by subtracting the net CH₄–N₂O effect shown in Equation 4 from the aboveground carbon accumulation curve published by (Robinson et al., 2024). To create global maps of potential carbon accumulation in naturally regenerating forests, Robinson et al. (2024) merged field measurements of carbon stocks with a comprehensive set of environmental factors. They then developed multiple random forest models to predict carbon accumulation across 5-year age intervals from 5 to 100 years. This approach generated predictions of potential carbon accumulation with a spatial resolution of approximately 1 km for the global terrestrial surface. Robinson et al. (2024) further refined the analysis, by fitting a Chapman-Richards growth curve to each pixel, thus creating global maps of the growth curve parameters. Refer to Robinson et al. (2024) for more details.

We note that this calculation does not include a number of factors that are necessary for an overall accounting of radiative forcing, including but not limited to soil CO₂ fluxes, belowground C storage, albedo, atmospheric sinks of CH₄ and N₂O, and GHGs aside from CO₂, CH₄, and N₂O (Weber et al., 2024).

2.4. Uncertainty Quantification of the CH₄–N₂O Effect of Regeneration Through Time

We quantified the propagation of uncertainty for the net CH₄–N₂O effect of regeneration through time using an analytical approach:

$$f(B_{0_br}, B_{1_br}) = B_{0_br} * t + \frac{B_{1_br} * t^2}{2} \quad (5)$$

$$\sigma_f = \sqrt{\left(\frac{\partial f}{\partial B_{0_br}} \sigma_{B_{0_br}}\right)^2 + \left(\frac{\partial f}{\partial B_{1_br}} \sigma_{B_{1_br}}\right)^2 + 2 \frac{\partial f}{\partial B_{0_br}} \frac{\partial f}{\partial B_{1_br}} \text{Cov}(B_{0_br}, B_{1_br})} \quad (6)$$

$$\sigma_f = \sqrt{(t \sigma_{B_{0_br}})^2 + \left(\frac{t^2}{2} \sigma_{B_{1_br}}\right)^2 + \frac{t^3}{2} \text{Cov}(B_{0_br}, B_{1_br})} \quad (7)$$

where t , B_{0_br} , and B_{1_br} are the same as described for Equation 3; The parameter $\sigma_{B_{0_br}}$ is the combined standard error of the back-transformed CH₄ and N₂O fixed-effect intercepts of the statistical models described in Equations 1 and 2, respectively (back-transformed to original unscaled units of Mg CO₂e ha^{−1} yr^{−1}), with $\sigma_{B_{0_br}} = \sqrt{\sigma_{B_{0_CH_4_br}}^2 + \sigma_{B_{0_N_2O_br}}^2}$ where $B_{0_CH_4_br}$ is the back-transformed CH₄ fixed-effect intercept and $B_{0_N_2O_br}$ N₂O is the back-transformed CH₄ fixed-effect intercept; The parameter $\sigma_{B_{1_br}}$ is the combined standard error of the back-transformed statistically significant CH₄ and N₂O coefficients of Age, the age of the ecosystem

(back-transformed from standardization to original units of years only if the B_1 coefficients were significant with $p < 0.1$, otherwise the age effect was treated as 0), with $\sigma_{B_{1_br}} = \sqrt{\sigma_{B_{1CH_4_br}}^2 + \sigma_{B_{1N_2O_br}}^2}$ where $B_{1CH_4_br}$ is the back-transformed CH_4 fixed-effect Age coefficient and $B_{1N_2O_br}$ is the back-transformed CH_4 fixed-effect Age coefficient; and $Cov(B_{0_{br}}, B_{1_{br}})$ is the variance-covariance matrix of the B_0 (intercept) and B_1 (ecosystem age) parameters of the gamma regression models described in Equations 1 and 2.

2.5. The “Climate Opportunity Benefits” of Regeneration Compared to Agriculture

For Q3, we defined the “climate opportunity benefit” of ecosystem regeneration as the subtraction of the mean net CH_4 - N_2O effect of agriculture from the net CH_4 - N_2O effect of regeneration. To compute the agricultural net CH_4 - N_2O effect, we leveraged the bottom-up CH_4 and N_2O inventory data for all agriculture-related categories available in the Emissions Database for Global Atmospheric Research (EDGAR) v8 global data set (Crippa et al., 2023). EDGAR is a multipurpose, independent, global database of anthropogenic emissions of GHGs and air pollution on Earth. EDGAR provides independent emission estimates compared to what reported by European Member States or by Parties under the United Nations Framework Convention on Climate Change, using international statistics and a consistent IPCC methodology. Using EDGAR data as opposed to relying on site-based studies comparing regenerating ecosystems to agricultural sites allowed us to have more flexibility to model these two land uses in a spatially explicit manner. Furthermore, there was a lack of information from most studies about previous agricultural land use. For example, less than half of the studies measuring fluxes in post-agriculture soils in our data set specified whether the prior agricultural land use was cropland or pasture (Table S2 in Supporting Information S1).

The EDGAR v8 categories in the compiled agricultural CH_4 inventory data set included: “Agricultural waste burning,” “Agricultural soils,” “Enteric fermentation,” and “Manure management.” We excluded CH_4 from rice cultivation because we wanted to maintain a closer comparison with the non-wetland ecosystems in our analysis. The categories in the agricultural N_2O data set included: “Agricultural waste burning,” “Agricultural soils,” “Indirect N_2O emissions from agriculture,” and “Manure management.” We summed all of the emissions from each category together for each year and subsequently computed the 2017–2022 mean agriculture CH_4 and N_2O fluxes (Figure S7 in Supporting Information S1).

We noticed that the gridded EDGAR agriculture CH_4 and N_2O data (Figure S8A in Supporting Information S1) reported emissions in numerous non-agriculture land cover classes as defined by the Terra and Aqua combined Moderate Resolution Imaging Spectroradiometer Land Cover Type (MCD12Q1) Version 6.1 data product (Friedl & Sulla-Menashe, 2022). We considered the emissions found in non-agriculture classes to be those outside the MCD12Q1 land cover classes of “croplands,” “cropland/natural vegetation mosaics,” and “grasslands” following the IGBP classification system. These fell into non-agriculture classes, including “open shrubland,” “closed shrubland,” and various forest and savanna classes. This suggested that the per unit area agricultural emissions of CH_4 and N_2O may be artificially low because the emissions were spatially distributed over a region larger than the actual extent of agriculture globally.

To address this issue, we spatially re-distributed all agricultural CH_4 and N_2O observations outside of IGBP cropland zones (i.e., pixels not categorized as “croplands” or “cropland/natural vegetation mosaics”) (Figure S8b in Supporting Information S1; see Eris Ely in revision). The IGBP land cover system does not differentiate between natural grasslands and pastures. We therefore defined pasture land by splitting the land area of grasslands between 57°N/S (Ramankutty et al., 2010) into natural versus cultivated per grid cell based on the estimate that cultivated pastures covered 26% of global grasslands in 2019 (FAO, 2023). Due to the latitude constraint ($\pm 57^\circ$ contains approximately 79% of global grasslands), this resulted in an effective pasture proportion of approximately 49.5% within the latitude bounds. The redistribution concentrated emissions from areas incorrectly allocated to non-agricultural land cover classes into these estimated pasture areas.

The final estimate of the CH_4 - N_2O effect from agriculture that we used to calculate the “opportunity benefit” of regeneration relative to agriculture consisted of the pasture land adjustment, the removal of areas with rice cultivation, and gap-filling of all NA pixels on naturally forest or savanna lands with the biome-specific means of the CH_4 - N_2O effect of agriculture (Figures S8c and S8d in Supporting Information S1). We used the gap-filling approach to estimate the “opportunity benefit” of regeneration in areas that are not currently agricultural but could be, thus allowing for an estimate in all forest and savanna ecosystems globally regardless of current land use. Gap-

filling with biome-specific mean values allowed us to provide a comprehensive global picture of the potential opportunity benefit of regeneration. This is a simplification, but it provides a useful approximation for evaluating the global climate opportunity benefit of regeneration.

The CH₄ and N₂O emissions from agriculture that we report have numerous uncertainties beyond those related to spatial allocation of pasture emissions. EDGAR estimation of emissions from the agricultural sector relies on activity data from FAOSTAT (FAO, 2023) and emission factors following Tier 1 of the IPCC Guidelines for National Greenhouse Gas Inventories (Eggleston et al., 2006). Information on key management practices that significantly affect emissions—such as fertilizer application methods, timing, and rates, manure management systems, and tillage practices—is often incomplete or missing from FAOSTAT databases. Relying on IPCC emissions factors introduces uncertainties caused by missing information on observance of agricultural laws and regulations (such as those related to handling and application of fertilizer and manure), and changing management practices in farming.

The emission factors have other large sources of uncertainty due to climate variability and variability within units that are assumed to be homogenous, such as spatial variability in a field or soil unit. Furthermore, the emissions from on-farm energy use, fertilizers manufacturing, pesticide manufacturing, food household consumption, food packaging, food processing, food transport, food retail, and food waste disposal are not included in our estimates of the CH₄ and N₂O emissions from agriculture. For more details, please refer to existing studies that quantify uncertainty for these bottom-up GHG inventories (Saunio et al., 2020; Solazzo et al., 2021; Tian et al., 2023).

3. Results

We analyzed data from 115 peer-reviewed studies that met our inclusion criteria ($n = 748$ plot-year observations; see SI). Our data set spanned all major biomes (Figure 1, Figure S1 in Supporting Information S1). Ecosystem ages ranged from 0 to >200 years, with a median age of 66 years.

Consistent with our expectations, subtropical/tropical savannas and forests were CH₄ sinks on average (Figures 2c and 2d, Table 1). The largest mean CH₄ sink was in subtropical/tropical savanna (-0.50 ± 0.05 Mg CO₂e ha⁻¹ yr⁻¹). Temperate conifer forests also tended toward being sinks (Figure 2A), though they were not clearly (Dushoff et al., 2019) different from zero. Boreal forests and temperate broadleaf forests were the only clear CH₄ sources (1.65 ± 1.07 and 0.78 ± 0.67 Mg CO₂e ha⁻¹ yr⁻¹, respectively).

All biomes acted as net N₂O sources, consistent with our expectations (Figure 2, Table 1). Temperate conifer forest was the largest N₂O source (1.00 ± 0.12 Mg CO₂e ha⁻¹ yr⁻¹), followed closely by temperate broadleaf forest (0.83 ± 0.16) and subtropical/tropical forest (0.78 ± 0.29), and subtropical/tropical savanna (0.65 ± 0.03).

We found modest support for a relationship between ecosystem age and GHG fluxes in some biome models (Table S3; Table S4 in Supporting Information S1). N₂O and CH₄ emissions tended to increase with ecosystem age. With each year increase in ecosystem age, N₂O emissions tended to increase by 0.018 ± 0.014 in temperate conifer forest, 0.016 ± 0.015 in temperate broadleaf forest, and 0.011 ± 0.011 Mg CO₂e ha⁻¹ yr⁻¹ in subtropical/tropical savanna ($p < 0.1$). CH₄ emissions tended to increase by 0.011 ± 0.011 Mg CO₂e ha⁻¹ yr⁻¹ in subtropical/tropical savanna ($p < 0.1$). However, note that most of the standard error values are nearly equal to the mean values of the age coefficients for both GHG models, indicating that these trends are noisy.

To compare the effects of CH₄ and N₂O to each other and to CO₂, we defined the “net CH₄-N₂O effect” to be the sum of the radiative forcing from CH₄ and N₂O in CO₂-equivalents (see Methods). A positive CH₄-N₂O effect indicates a net warming effect on the climate, whereas a negative CH₄-N₂O effect indicates a net cooling effect. The net CH₄-N₂O effect was positive (net warming) across all biomes (Figures 2 and 3, Figure S3 in Supporting Information S1). Three of the five biomes followed our expectation of an N₂O source outweighing a CH₄ sink or a trend toward a CH₄ sink, yielding a net warming CH₄-N₂O effect: subtropical/tropical forest, subtropical/tropical savanna and temperate conifer forest (0.60 ± 0.30 , 0.15 ± 0.06 , and 0.83 ± 0.24 Mg CO₂e ha⁻¹ yr⁻¹, respectively) (Table 2). The global mean among all biomes shows the overall pattern of a net warming CH₄-N₂O effect characterized by a positive N₂O source outweighing a smaller—in this case not clearly negative—CH₄ effect (Figure 2f). Boreal and temperate broadleaf forests also had net warming CH₄-N₂O effects (1.83 ± 1.07 and 1.61 ± 0.69 Mg CO₂e ha⁻¹ yr⁻¹, respectively), but unlike the other biomes, this was driven by both a CH₄ source and an N₂O source.

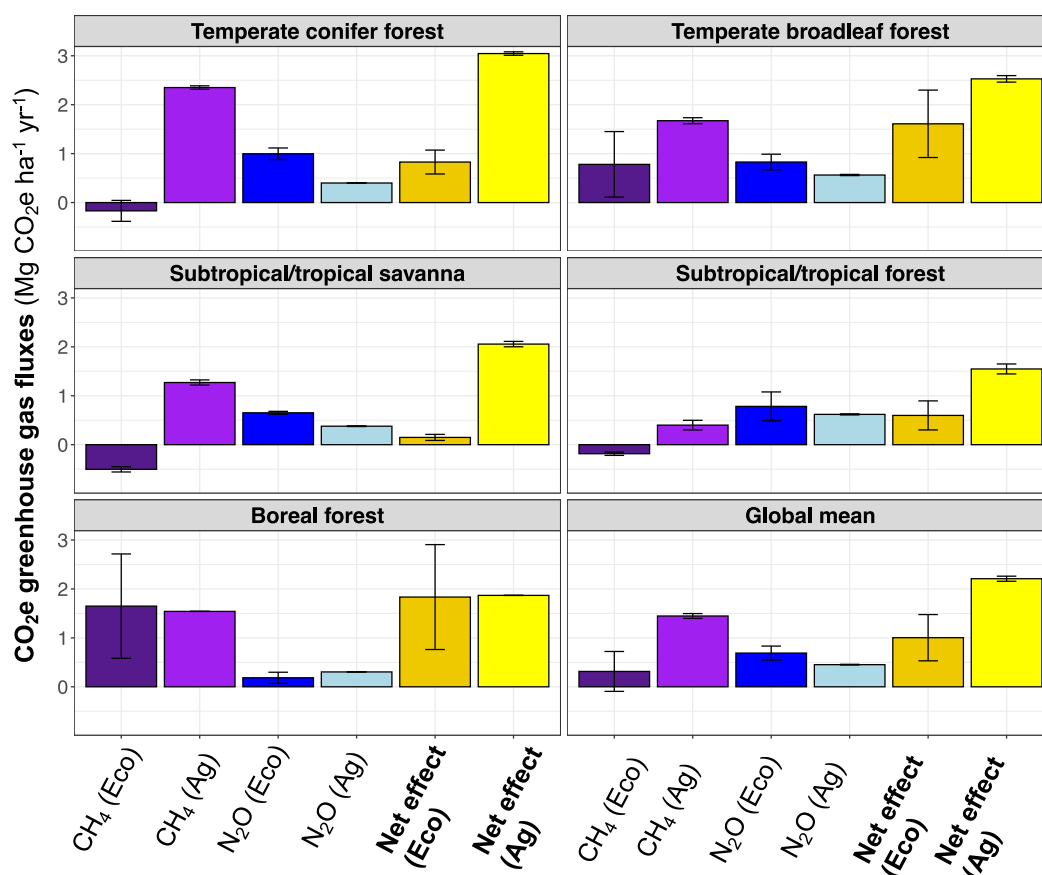


Figure 2. The modeled intercept and standard error of the CH₄ (purple), N₂O (blue) and net CH₄–N₂O (yellow) effects of ecosystem regeneration (“Eco,” dark colors) compared to agriculture (“Ag,” light colors) are shown for (a) temperate conifer forest, (b) temperate broadleaf forest, (c) subtropical/tropical savanna, (d) subtropical/tropical forest, (e) boreal forest, and (f) global means. Modeled intercepts for ecosystem regeneration show the expected fluxes of an average-aged forest in biome-averaged environmental conditions (see details in Methods). Error bars for agriculture show the biome-specific standard deviation of annual agricultural fluxes using a 5-year baseline of 2017–2022 (Figure S7 in Supporting Information S1). Positive values indicate warming effects (i.e., sources of CH₄ or N₂O), whereas negative values indicate cooling effects (i.e., sinks of CH₄ or N₂O).

Presenting the biome-specific GHG flux model results on a map (Figure 3) allows us to visualize the net CH₄–N₂O effects in forests and savannas across the globe. The net N₂O source outweighs the net CH₄ sink in most biomes, leading to a 9.65 ± 7.26 Pg CO₂e yr⁻¹ net warming effect among all forested and savanna biomes globally.

The IPCC Sixth Assessment accounted for the direct CO₂ sequestration from biomass accumulation during regeneration and its radiative cooling effect on the climate (IPCC, 2022). However, CH₄ and N₂O fluxes from unmanaged ecosystems were not considered. To address this gap, we explored the implications of our results in the context of the global climate mitigation assessments for ecosystem regeneration. We leveraged a novel aboveground biomass data set published by Robinson et al. (2024) (see Methods) to assess how the CH₄–N₂O effect impacts our global understanding of the climate benefits of regeneration. The data from Robinson et al. (2024) reveal that subtropical/tropical forests have the highest rates of aboveground carbon accumulation, averaging 52.4 Mg CO₂e ha⁻¹ yr⁻¹ after 50 years of regeneration. This is followed by temperate broadleaf forests (29.0 Mg CO₂e ha⁻¹ yr⁻¹), temperate conifer forests (22.33 Mg CO₂e ha⁻¹ yr⁻¹), subtropical/tropical savanna (26.1 Mg CO₂e ha⁻¹ yr⁻¹), and boreal forests with the lowest accumulation rate (17.4 Mg CO₂e ha⁻¹ yr⁻¹).

Our results suggest that after 50 years of regeneration, the net CH₄–N₂O effect reduces the CO₂ sequestration benefits from aboveground biomass accumulation by 50% on average globally (Figure 4). Yet even after 100 years of regeneration, the radiative cooling of the climate from aboveground CO₂ sequestration still exceeds the radiative warming driven by the net CH₄–N₂O effect among most ecosystems (with the exception of boreal

Table 1

Summary of the Biome-Specific Model Results for Predicting Mean CH₄ and N₂O Fluxes for Boreal, Subtropical/Tropical Savanna, Subtropical/Tropical Moist, Temperate Conifer, and Temperate Broadleaf Biomes

Biome	n obs [num. Plot-years]	N pub [num. Studies]	CH ₄ intercept [Mg CO ₂ e ha ⁻¹ yr ⁻¹]	CH ₄ standard error	n obs [num. Plot-years]	N pub [num. Studies]	N ₂ O intercept [Mg CO ₂ e ha ⁻¹ yr ⁻¹]	N ₂ O standard error
Temperate conifer forest	44	8	-0.17	0.21	22	5	1.00	0.12
Temperate broadleaf forest	259	37	0.78	0.67	210	37	0.83	0.16
Subtropical/tropical savanna	24	6	-0.50	0.05	20	5	0.65	0.03
Subtropical/tropical forest	41	10	-0.18	0.03	81	13	0.78	0.29
Boreal forest	92	12	1.65	1.07	59	5	0.19	0.11

Note. The back-transformed model intercept (mean CH₄ and N₂O evaluated with other coefficients are equal to their means) and standard error values are reported in CO₂-equivalent units of Mg CO₂e ha⁻¹ yr⁻¹.

and high-latitude temperate broadleaf forests). We also found that the radiative effects of agriculture from CH₄ and N₂O fluxes are more warming than the radiative effects of regeneration (including C sequestration in aboveground biomass as well as CH₄ and N₂O fluxes) among all ecosystems spanning the same 100-year timeframe (Figure 4).

In temperate broadleaf forests, the net CH₄-N₂O effect from regeneration begins to outweigh the cooling effect from aboveground biomass accumulation after 75 years of regrowth (Figure 4b). Similarly, in boreal forests, with the second highest mean net CH₄-N₂O effect from regeneration, the radiative warming driven by the net CH₄-N₂O effect from regeneration begins to outweigh the cooling effect from aboveground biomass accumulation after 62 years of regeneration (Figure 4e). Even in this case, where Boreal forest has the lowest mean net CH₄-N₂O effect from agriculture among all other biomes, our model suggests that the radiative effects of agriculture are more warming than the radiative effects of regeneration over 100 years.

The net warming CH₄-N₂O effect in most natural biomes lessens the climate benefits of ecosystem regeneration by 236.3 Mg CO₂e ha⁻¹ yr⁻¹ on average globally spanning a 100-year timeframe. This amounts to about 0.6% of global CO₂ emissions from all energy combustion and industrial processes in 2022 (IEA, 2023). To explicitly take into account the climate costs of alternate land uses, we compared a counterfactual of the net CH₄-N₂O effect of cropland and pasture to the net CH₄-N₂O effect of forest regeneration that we calculated in the meta-analysis (Figure 5). We defined the net CH₄-N₂O effect from agriculture to be the sum of the 2017–2022 mean CH₄ and N₂O fluxes from agriculture (Figure 5, Figure S7 in Supporting Information S1) based on the EDGAR v8 bottom-up CH₄ and N₂O inventory data for all agriculture-related categories (Crippa et al., 2023). The hotspots from the agriculture CH₄-N₂O effect mostly correspond to areas of animal agriculture (since rice cultivation was removed).

Accounting for the CH₄ and N₂O emissions from agriculture highlights that in most regions, ecosystem regeneration remains a meaningful climate mitigation strategy, with a lower net CH₄-N₂O effect relative to the emissions from current agricultural practices. In comparison to agriculture, we found that unmanaged ecosystem regeneration in most regions of the globe provides a “climate opportunity benefit” (defined as the subtraction of the mean net CH₄-N₂O effect of agriculture from the CH₄-N₂O effect of regeneration, Figure 5). The largest climate opportunity benefits of regeneration averaged 1.83 and 1.75 Mg CO₂e ha⁻¹ yr⁻¹ of net cooling relative to agricultural land use in tropical/subtropical forest and temperate broadleaf forest, respectively (Figure 5b). The large warming effect from boreal regions reflects the relatively low agricultural emissions reported in this region compared to the net CH₄-N₂O effect of boreal forest regeneration, though emissions might increase as future warming conditions allow for more agricultural activity and different management practices in this region (Jägermeyr et al., 2021; King et al., 2018).

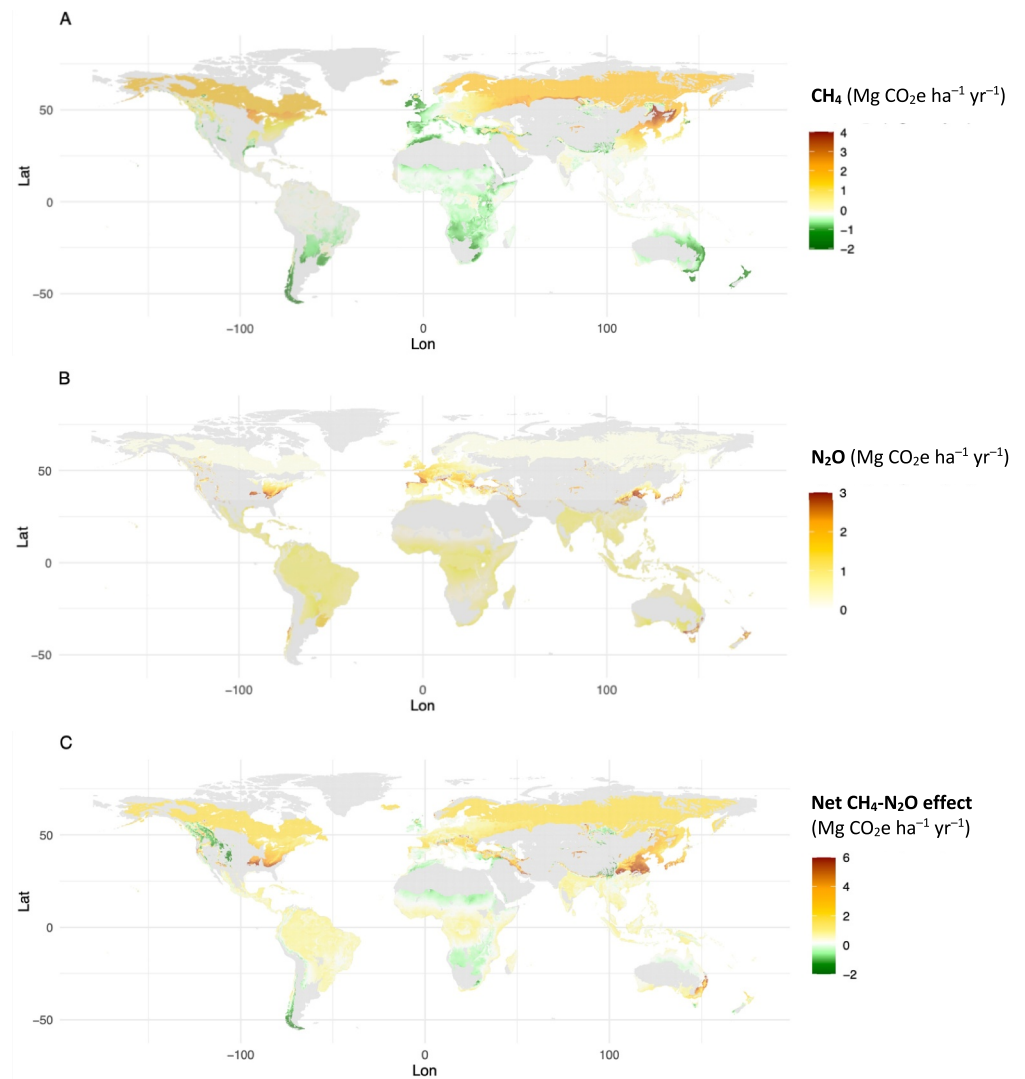


Figure 3. Global estimates of the (a) CH_4 , (b) N_2O and (c) net $\text{CH}_4\text{-N}_2\text{O}$ effects of ecosystem regeneration from the best performing gamma regression models for each biome (same models as results in Figure 2, Table 1 and Table S3 in Supporting Information S1).

Table 2

Mean and Standard Error of the Net $\text{CH}_4\text{-N}_2\text{O}$ Effect of Ecosystem Regeneration Among Biomes

Biome	Net $\text{CH}_4\text{-N}_2\text{O}$ effect ($\text{Mg CO}_2\text{e ha}^{-1} \text{yr}^{-1}$)	Standard error
Temperate conifer forest	0.83	0.24
Temperate broadleaf forest	1.61	0.69
Subtropical/tropical grassland and savanna	0.15	0.06
Subtropical/tropical forest	0.60	0.30
Boreal forest	1.83	1.07

Note. The net $\text{CH}_4\text{-N}_2\text{O}$ effects and standard error values are reported in CO_2 -equivalent units of $\text{Mg CO}_2\text{e ha}^{-1} \text{yr}^{-1}$.

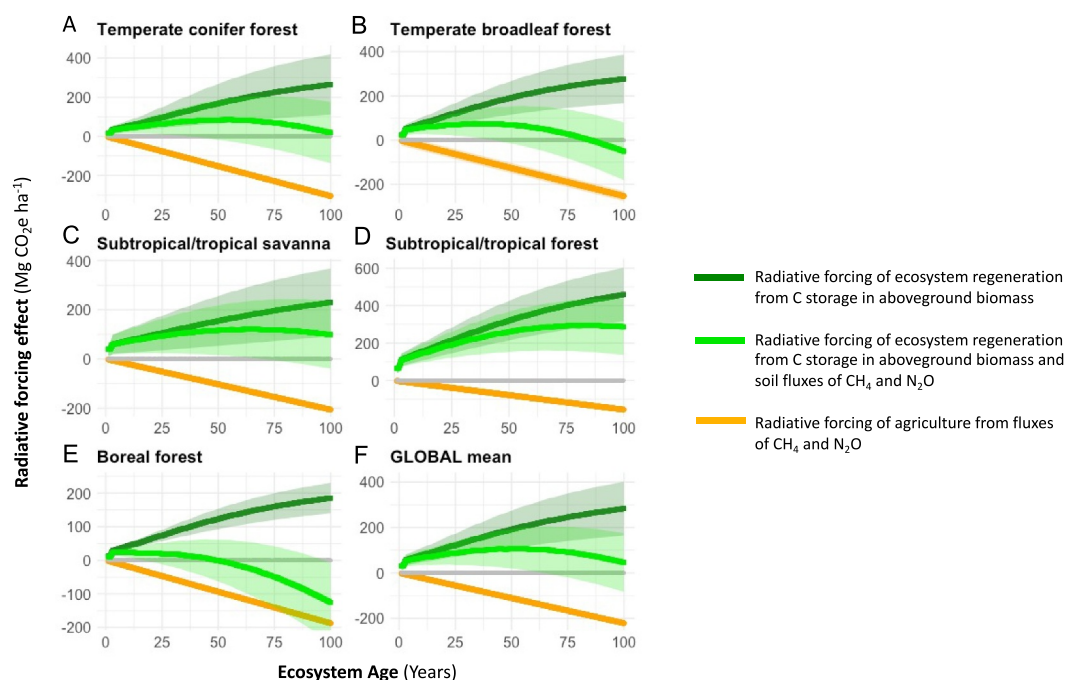


Figure 4. Differences between radiative forcing effects of ecosystem regeneration with and without taking into account CH₄ and N₂O fluxes for (a) temperate conifer forest, (b) temperate broadleaf forest, (c) subtropical/tropical savanna, (d) subtropical/tropical forest, (e) boreal forest, and (f) global means. The gray line at zero is the balance between cooling (positive) and warming (negative) radiative forcing effects (note the change in sign convention from Figures 2, 3 and 5 to be consistent with published studies focused on aboveground CO₂ sequestration including Cook-Patton et al., 2020; Robinson et al., 2024). The dark green curves (means) and shading (±1 SD) show CO₂ sequestration during aboveground biomass accumulation from regeneration, using estimates from Robinson et al. (2024). The light green curves show the combination of CO₂ sequestration in aboveground biomass and the radiative forcing of the net CH₄–N₂O effect. Orange curves show the net CH₄–N₂O effect of agriculture. The agriculture-related emissions were based on the mean EDGARv8 estimates during 2017–2022 (Figure S7 in Supporting Information S1) and were assumed to be constant over the 100-year time frame. Note that we did not consider sequestered CO₂ from cropland aboveground biomass or changes in soil C sequestration.

4. Discussion

4.1. Spotlight of Key Results

We found that most regenerating ecosystems act as small CH₄ sinks and relatively larger N₂O sources, with a net warming combined CH₄–N₂O effect for all biomes (Q1). Yet even after 100 years of regeneration, the radiative cooling of the climate from aboveground CO₂ sequestration exceeds the radiative warming driven by the net CH₄–N₂O effect among all ecosystems on average globally (Q2). Furthermore, the results suggest that the “climate opportunity benefit” of ecosystem regeneration yields a net cooling effect for all biomes relative to agriculture when considering the same 100-year period of regeneration (Q3).

Although substantial in magnitude, the global net CH₄–N₂O warming effect we estimate from natural forests and savannas (9.65 ± 7.26 Pg CO₂e yr⁻¹) is considerably smaller than the total global anthropogenic net CH₄–N₂O emissions from fossil fuel burning, industry and agriculture. These anthropogenic sources emit 31.32 (95% confidence limits 29.51–34.94) Pg CO₂e yr⁻¹, with anthropogenic gross N₂O emissions contributing 1.94 (0.95–2.98) Pg CO₂e yr⁻¹ (Tian et al., 2023) and gross CH₄ emissions contributing 29.38 (28.56–31.96) Pg CO₂e yr⁻¹ (Saunio et al., 2020).

Even after accounting for CH₄ and N₂O fluxes, we found that the climate benefits (i.e., radiative cooling effect) of keeping mature forests intact exceed the alternative of deforestation in all biomes. This finding extends our understanding of the net radiative effects across succession (Q1) by highlighting the importance of preserving existing forest carbon stocks. Our results showed that ecosystem age had modest and, in some cases, not clearly positive or negative effects on CH₄ and N₂O fluxes among most biomes (Table S3 in Supporting Information S1). This suggests that cutting down a forest generally results in CH₄ and N₂O fluxes during early succession—after

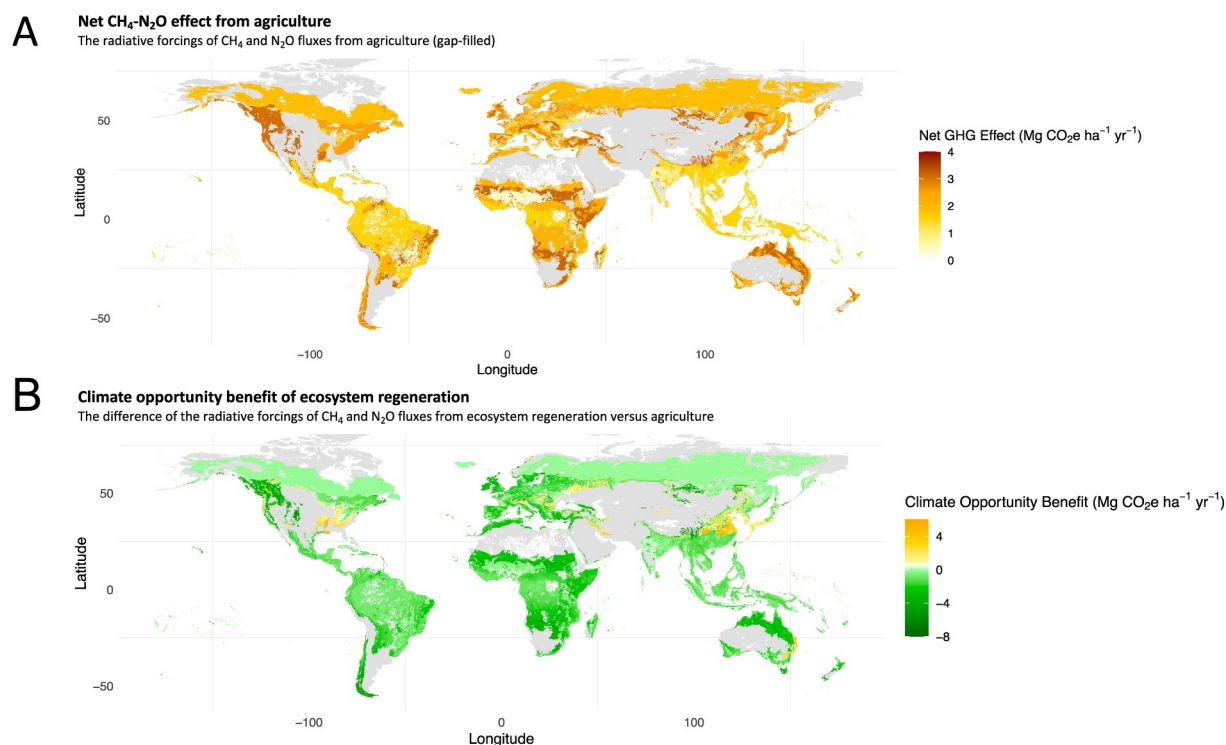


Figure 5. Global maps of (a) the net CH₄–N₂O effect in CO₂-equivalent flux per unit of agricultural land per year from the original Emissions Database for Global Atmospheric Research v8 inventory data (most values are identical to Figure S8C in Supporting Information S1 with remaining NA pixels within regeneration extent gap-filled using S3 biome-mean values shown in Figure S8d in Supporting Information S1), and (b) the “climate opportunity benefit” (i.e., the agriculture-adjusted CH₄–N₂O effect) of ecosystem regeneration defined as the subtraction of the mean net CH₄–N₂O effect of agriculture from the CH₄–N₂O effect of regeneration. The opportunity benefit calculation subtracts agricultural effects from regeneration effects for all areas where regeneration predictions exist. Prior to calculating the mean agriculture estimates used in (b), we removed CH₄ from rice cultivation (shown as dark red areas in (a) and adjusted for artificially low pasture fluxes (see Methods and Figure S8 in Supporting Information S1).

the typical initial high pulse of post-disturbance CH₄ and N₂O emissions immediately following many disturbance events (Pugh et al., 2019; Tian et al., 2015)—that are similar in magnitude to fluxes from the prior mature forest. This relatively stable pattern of non-CO₂ greenhouse gas fluxes further supports our finding that above-ground CO₂ sequestration benefits dominate the net radiative effect of regeneration (Q2).

4.2. Drivers of GHG Fluxes Among Biomes

The observed variations in CH₄ and N₂O fluxes across biomes reflect complex interactions between climate conditions, soil properties, and ecosystem processes that control greenhouse gas production, consumption, and transport. In tropical and subtropical ecosystems, soil texture (particularly % sand) and topographic variables like slope and elevation were more influential than precipitation metrics, possibly due to their effects on soil aeration and gas diffusivity. These well-drained conditions favor methanotrophy, explaining the CH₄ sink behavior observed in these upland tropical regions (Vasconcelos et al., 2004). Conversely, high-latitude ecosystems including temperate broadleaf and boreal forests showed different patterns where temperature variables strongly influenced CH₄ dynamics, consistent with seasonal freeze-thaw cycles in boreal systems creating microsite anoxia conducive to methanogenesis (Borken & Brumme, 2009).

For N₂O emissions, temperature-related variables consistently ranked highly across biomes, possibly reflecting the temperature sensitivity of microbial nitrification and denitrification processes (Dobbie & Smith, 2001; Koponen & Martikainen, 2004). Soil properties, particularly clay content in temperate conifer forests, clearly affected GHG fluxes, possibly through influencing water retention and creating heterogeneous oxygen conditions (Davidson et al., 2000). These biome-specific relationships raise important considerations for interpretation of underrepresented regions—such as tropical forest and savanna ecosystems—as well as extrapolation to other ecosystems not included in the study—such as montane tropical forests or Mediterranean ecosystems—which

might exhibit distinctive and more nuanced GHG flux patterns driven by unique combinations of environmental factors. Furthermore, as climate change alters temperature and precipitation regimes globally (Kharin et al., 2013), the relative importance of these controlling factors may shift, potentially altering future GHG flux patterns and the climate mitigation potential of forest regeneration across biomes.

4.3. The Importance of Mature Forest Conservation

While our analysis focused on regenerating systems, our findings include results from mature forests as well. Despite their low net ecosystem productivity, old-growth forests act as long-term carbon reservoirs. Deforestation causes the release of CO₂ into the atmosphere that otherwise would remain stored in forest biomass that, under stable forest conditions (i.e., low disturbance rates), can be retained for longer than three centuries in some ecosystems (Martin-Benito et al., 2021). This long-term storage capacity reinforces the importance of our finding that natural forest ecosystems provide greater climate benefits than agricultural alternatives (Q3). However, many forests—including tropical ecosystems with the greatest aboveground CO₂ sequestration potential among all biomes—are experiencing disturbances at more frequent timescales (Schwartz et al., 2020; Taubert et al., 2018). Increasing disturbances in old-growth forests release large amounts of stored carbon that can take centuries to recover (Martin-Benito et al., 2021; Pugh et al., 2019) or that may not recover at all under current and future climate change (Esquivel-Muelbert et al., 2020; McDowell et al., 2022; Parsons, 2020). This vulnerability highlights the urgency of protecting existing forests while also pursuing the regeneration opportunities identified in our study.

The climate importance of mature forest conservation is further supported by research on soil carbon dynamics. Soils in old-growth forests store carbon longer than in more disturbed forests (Knohl et al., 2003; Luyssaert et al., 2008). These old-growth forest soil C reservoirs have particularly important climate implications under the ongoing decrease of turnover times in living vegetation forest carbon attributed to CO₂ enrichment as well as changes in temperature and precipitation patterns (Schwartz et al., 2020; Yu et al., 2019). Furthermore, a recent study in Southeast Asia showed that secondary forests can have greater soil C efflux rates than old-growth forests, suggesting that conversion of old-growth forests into secondary forests may drive greater C loss from soils even after 70 years of regrowth (Raczka et al., 2023).

4.4. Climate Policy Recommendations

Our findings on the climate opportunity benefits of ecosystem regeneration have important implications for climate policy that must be communicated carefully to avoid misinterpretation. We recommend three policy approaches based on the combination of our results and other studies to ensure that ecosystem regeneration is appropriately valued and implemented alongside emission reductions:

4.4.1. Adopt a “Both/And” Framework for Climate Action

Our research demonstrates that regenerating ecosystems provide a net cooling benefit compared to agricultural alternatives, but this benefit is fundamentally different from and cannot substitute for reducing fossil fuel emissions. Climate policies could explicitly recognize the distinct and complementary roles of ecosystem regeneration and emission reductions. Article 5 of the Paris Agreement provides a foundation for this approach by encouraging both conservation and enhancement of carbon sinks alongside emissions reductions, but implementation requires stronger guardrails. Furthermore, voluntary carbon markets require fundamental reform to prevent the use of nature-based carbon credits as a substitute for emission reductions. This includes establishing stricter additionality requirements, longer permanence periods, prevention of offsetting claims and the establishment of public funding for ecosystem regeneration that operates independently from carbon markets. Direct payments for ecosystem services, tax incentives for plant-based diets, public conservation funds, and green recovery investments can support regeneration without enabling continued fossil fuel emissions.

4.4.2. Improve Carbon Accounting Methodologies

Accurate carbon accounting methodologies must include the full climate implications of ecosystem regeneration, including non-CO₂ GHGs as demonstrated in our study, as well as changes in surface albedo and ozone emissions (Weber et al., 2024), plant-mediated CH₄ fluxes (Covey & Megonigal, 2019; Gauci et al., 2024), and below-ground carbon storage (Jones et al., 2019; Terrer et al., 2021; Usuga et al., 2010).

Furthermore, accounting for emissions from agricultural land use as a counterfactual to regeneration provides a critical foundation for informed climate-friendly land use policies. Our findings on the climate costs of agriculture contribute to a growing body of work focusing on the benefits of dietary shifts that reduce demand for animal agriculture and create opportunities for ecosystem regeneration (Hayek et al., 2020). To support just transitions, climate policies must include measures to support agricultural communities in transitioning to more sustainable practices or alternative livelihoods.

4.4.3. Align With Local Contexts and Prioritize High-Benefit Regions for Regeneration

Our findings on spatial variation in climate opportunity benefits can inform the strategic prioritization of regeneration efforts, particularly in tropical and subtropical regions where we found the largest opportunity benefits. This spatial prioritization could integrate into national climate plans and biodiversity strategies to maximize cross-cutting benefits while aligning with local contexts and priorities. The European Union's Nature Restoration Law and similar initiatives worldwide provide models for ecological restoration that emphasize multiple benefits beyond carbon sequestration.

Research demonstrates that forests remain intact longer and store more carbon when Indigenous Peoples have secure land rights and management authority (Sze et al., 2022; Townsend et al., 2020). Effective ecosystem regeneration initiatives recognize Indigenous Peoples' sovereignty, secure their land rights, and integrate Indigenous knowledge systems (Ban et al., 2018; Dawson et al., 2021; Donkor & Marns, 2022; González & Kröger, 2020).

5. Limitations

As is common in meta-analyses (Gurevitch et al., 2018), the study sites with published CH₄ and N₂O fluxes are not randomly selected across space, with clusters in North America, Western Europe, and East Asia. This spatial bias limits our ability to make robust inferences about underrepresented regions with relatively few measurements, including South America, Africa, Australia, and Southeast Asia. Furthermore, our data set includes studies that were conducted using a range of methodologies for quantifying CH₄ and N₂O fluxes, with differences in sampling protocol, chamber design, and emission rate calculation. Such methodological differences cause uncertainty in the magnitude of flux estimates. While our mixed-effects modeling approach accounts for some of this variability by including the study as a random effect, it cannot fully eliminate the influence of methodological differences. There is high variability in the CH₄ and N₂O fluxes (Figures S2, S3 in Supporting Information S1)—both across sites and within a given site, even within a single day of data collection (Anthony & Silver, 2021; Castaldi et al., 2013; Groffman et al., 2009; Lawrence et al., 2021). The high variability of CH₄ and N₂O fluxes through space (“hot spots”) and time (“hot moments”) further underscores the need for additional GHG flux measurements, particularly in regions with low data availability (South America, Africa, Australia and Southeast Asia). While our model selection approach optimized performance for each biome-gas combination, some models still included covariates with relatively high p-values or lacked important drivers known to influence greenhouse gas fluxes, such as high-resolution soil moisture data. Our sensitivity analysis (Table S5 in Supporting Information S1) revealed that some model results, particularly for N₂O in boreal forests, showed considerable variability depending on the modeling choices, highlighting the uncertainty in these estimates.

Our reliance on the EDGAR inventory data for agricultural emissions introduces several additional uncertainties due to the limitations of Tier 1 IPCC emission factors and the challenges in accurately distributing emissions spatially (see Methods). First, Tier 1 emission factors represent highly generalized estimates designed for global application and do not capture the substantial variability in emission rates due to local environmental conditions, management practices, and agricultural technologies. This generalization likely underestimates both the spatial and temporal variability of emissions, potentially smoothing out emission hotspots. In regions with intensive agricultural practices that exceed typical emission factors, we may underestimate the climate benefits of regeneration. Conversely, in regions with more sustainable agricultural practices than assumed in Tier 1 factors, the benefits might be overestimated. In general, our estimates of agricultural emissions in most regions are likely to be conservative, which could lead to underestimation of the climate opportunity benefit of regeneration in these areas. Second, the quality of the data used for scaling emissions varies considerably by region and agricultural practice. Third, our spatial redistribution of agricultural emissions outside IGBP cropland zones required assumptions about the distribution of pasture lands. While we based this on the best available global estimates (26%

of global grasslands as cultivated pastures (FAO, 2023)), actual proportions vary widely by region and are not well characterized in many areas. The spatial redistribution uncertainties further complicate regional comparisons, although global patterns remain robust. Overall, these limitations suggest that our estimates of climate opportunity benefits from regeneration relative to agriculture should be interpreted as conservative approximations, with the understanding that site-specific assessments would be necessary for more precise local estimates.

6. Conclusion

This study provides insights into the global climate mitigation potential of ecosystem regeneration. We found that regenerating mid- and low-latitude forest and savanna ecosystems tend to produce net warming effects from the combination of CH₄ and N₂O, typically because N₂O sources outweigh small CH₄ sinks. The balance between these two contrasting effects allows for a more comprehensive understanding of the climate impacts of ecosystem regeneration. Our results suggest that the “climate opportunity benefit” of ecosystem regeneration—meaning the avoided emissions by not converting these ecosystems into agricultural land—generally outweighs the warming effects of agricultural CH₄ and N₂O emissions, with the largest relative gains in the tropics. This result lends itself to further analysis. For example, our findings could be subsequently assessed based on land use scenarios of increased plant-based diets compared to the business-as-usual levels of animal agriculture, leveraging existing work that quantifies the C “opportunity cost” of animal-sourced food production globally (Hayek et al., 2020). Our findings promote ecosystem regeneration as a climate action that, in synergy with aggressive reductions in fossil fuel emissions, can foster many co-benefits such as support of sustainable livelihoods and protection of biodiversity.

Data Availability Statement

Our data and code used for analysis are publicly available. The data we extracted for our meta-analysis, including the DOIs for each peer-reviewed publication from which all data were extracted, are publicly available on FigShare (Cooley et al., 2024). Statistical analyses were conducted with R version 4.4.3 (R Core Team, 2024) using the robustlmm package (Koller, 2016). Figures were made with ggplot2 package version 3.5.2 (Wickham et al., 2025). The code used to conduct statistical analyses and create figures is publicly available on GitHub: https://github.com/savcooley/ch4_metaAnalysis_public.git.

Acknowledgments

We thank Nathaniel Robinson and Susan Cook-Patton for sharing their data. We thank Ayanna Butler for her contributions in the initial conceptualization of this study. We thank Ruby An for sharing her expertise and suggestions about Boreal ecosystems. We thank Evelyn Beaur, Jeffrey Smith and the other members of the Levine Lab at Princeton University for their feedback. We thank the Department of Ecology, Evolution and Environmental Biology, Columbia University for funding the majority of this research. We thank the Columbia University Climate School for also providing financial support for this research. A portion of this research was carried out at the Jet Propulsion Laboratory, California Institute of Technology, under a contract with the National Aeronautics and Space Administration (NASA). Government sponsorship is acknowledged.

References

- Abernethy, S., & Jackson, R. B. (2022). Global temperature goals should determine the time horizons for greenhouse gas emission metrics. *Environmental Research Letters*, 17(2), 024019. <https://doi.org/10.1088/1748-9326/ac4940>
- Anthony, T. L., & Silver, W. L. (2021). Hot moments drive extreme nitrous oxide and methane emissions from agricultural peatlands. *Global Change Biology*, 27(20), 5141–5153. <https://doi.org/10.1111/gcb.15802>
- Aronson, E., & Allison, S. (2012). Meta-analysis of environmental impacts on nitrous oxide release in response to N amendment. *Frontiers in Microbiology*, 3, 272. <https://doi.org/10.3389/fmicb.2012.00272>
- Ban, N. C., Frid, A., Reid, M., Edgar, B., Shaw, D., & Siwallace, P. (2018). Incorporate Indigenous perspectives for impactful research and effective management. *Nature Ecology & Evolution*, 2(11), 1680–1683. <https://doi.org/10.1038/s41559-018-0706-0>
- Borchard, N., Schirrmann, M., Cayuela, M. L., Kammann, C., Wrage-Mönnig, N., Estavillo, J. M., et al. (2019). Biochar, soil and land-use interactions that reduce nitrate leaching and N₂O emissions: A meta-analysis. *Science of The Total Environment*, 651, 2354–2364. <https://doi.org/10.1016/j.scitotenv.2018.10.060>
- Borken, W., & Brumme, R. (2009). Methane uptake by temperate forest soils. In K. Brumme & B. E. Khanna (Eds.), *Functioning and Management of European Beech Ecosystems* (pp. 369–381). Springer. https://doi.org/10.1007/b82392_20
- Brümmer, C., Brüggemann, N., Butterbach-Bahl, K., Falk, U., Szarzynski, J., Vielhauer, K., et al. (2008). Soil-atmosphere exchange of N₂O and NO in near-natural savanna and agricultural land in Burkina Faso (West Africa). *Ecosystems*, 11(4), 582–600. <https://doi.org/10.1007/s10021-008-9144-1>
- Butterbach-bahl, K., & Papen, H. (2002). Four years continuous record of CH₄-exchange between the atmosphere and untreated and limed soil of a N-saturated spruce and beech forest ecosystem in Germany. *Plant and Soil*, 240(1), 77–90. <https://doi.org/10.1023/A:1015856617553>
- Castaldi, S., Bertolini, T., Valente, A., Chiti, T., & Valentini, R. (2013). Nitrous oxide emissions from soil of an African rain forest in Ghana. *Biogeosciences*, 10(6), 4179–4187. <https://doi.org/10.5194/bg-10-4179-2013>
- Chazdon, R. L. (2003). Tropical forest recovery: Legacies of human impact and natural disturbances. *Perspectives in Plant Ecology, Evolution and Systematics*, 6(1), 51–71. <https://doi.org/10.1078/1433-8319-00042>
- Cook-Patton, S. C., Leavitt, S. M., Gibbs, D., Harris, N. L., Lister, K., Anderson-Teixeira, K. J., et al. (2020). Mapping carbon accumulation potential from global natural forest regrowth. *Nature*, 585(7826), 545–550. <https://doi.org/10.1038/s41586-020-2686-x>
- Cooley, S. S., Moore, E., Martinez, J., Fahlen, J., Maybach, E., Gollerkeri, M., et al. (2024). Cooley_et_al_data_Agg_Nov2024_dP.csv [Dataset]. *figshare*. <https://doi.org/10.6084/M9.FIGSHARE.27923028>
- Covey, K. R., & Megonigal, J. P. (2019). Methane production and emissions in trees and forests. *New Phytologist*, 222(1), 35–51. <https://doi.org/10.1111/nph.15624>
- Crippa, M., Guizzardi, D., Pagani, F., Schiavina, M., Melchiorri, M., Pisoni, E., et al. (2023). Insights on the spatial distribution of global, national and sub-national GHG emissions in EDGARv8.0. *Earth System Science Data Discussions*, 1–28. <https://doi.org/10.5194/essd-2023-514>

- Danielson, J. J., & Gesch, D. B. (2011). Global multi-resolution terrain elevation data 2010 (GMTED2010) [Dataset]. *USGS Open-File Report 2011-1073*. <http://pubs.usgs.gov/of/2011/1073/>
- Davidson, E. A., Keller, M., Erickson, H. E., Verchot, L. V., & Veldkamp, E. (2000). Testing a conceptual model of soil emissions of nitrous and nitric oxides: Using two functions based on soil nitrogen availability and soil water content, the hole-in-the-pipe model characterizes a large fraction of the observed variation of nitric oxide and nitrous oxide emissions from soils. *BioScience*, 50(8), 667–680. [https://doi.org/10.1641/0006-3568\(2000\)050\[0667:TACMOS\]2.0.CO;2](https://doi.org/10.1641/0006-3568(2000)050[0667:TACMOS]2.0.CO;2)
- Dobbie, K. E., & Smith, K. A. (2001). The effects of temperature, water-filled pore space and land use on N₂O emissions from an imperfectly drained gleysol. *European Journal of Soil Science*, 52(4), 667–673. <https://doi.org/10.1046/j.1365-2389.2001.00395.x>
- Donkor, F. K., & Mearns, K. (2022). Harnessing Indigenous knowledge systems for enhanced climate change adaptation and governance: Perspectives from Sub-Saharan Africa. In *Indigenous knowledge and climate governance: A Sub-Saharan African perspective* (pp. 181–191). Springer International Publishing.
- Dushoff, J., Kain, M. P., & Bolker, B. M. (2019). I can see clearly now: Reinterpreting statistical significance. *Methods in Ecology and Evolution*, 10(6), 756–759. <https://doi.org/10.1111/2041-210X.13159>
- Dutaur, L., & Verchot, L. V. (2007). A global inventory of the soil CH₄ sink. *Global Biogeochemical Cycles*, 21(4). <https://doi.org/10.1029/2006GB002734>
- Dawson, N. M., Coolsaet, B., Sterling, E. J., Loveridge, R., Gross-Camp, N. D., Wongbusarakum, S., et al. (2021). The role of Indigenous peoples and local communities in effective and equitable conservation. *Ecology and Society*, 26(3). <https://doi.org/10.5751/ES-12625-260319>
- Eggleston, H. S., Buendia, L., Miwa, K., Ngara, T., & Tanabe, K. (2006). IPCC guidelines for national greenhouse gas inventories. Retrieved from <https://www.osti.gov/etdweb/biblio/20880391>
- Esquivel-Muelbert, A., Phillips, O. L., Brien, R. J. W., Fauset, S., Sullivan, M. J. P., Baker, T. R., et al. (2020). Tree mode of death and mortality risk factors across Amazon forests. *Nature Communications*, 11(1), 5515. <https://doi.org/10.1038/s41467-020-18996-3>
- FAO. (2023). Faostat - Food and agriculture organization of the United Nations. Retrieved from <https://www.fao.org/faostat/en/#data/GT>
- Feng, Z., Wang, L., Wan, X., Yang, J., Peng, Q., Liang, T., et al. (2022). Responses of soil greenhouse gas emissions to land use conversion and reversion—A global meta-analysis. *Global Change Biology*, 28(22), 6665–6678. <https://doi.org/10.1111/gcb.16370>
- Fest, B., Wardlaw, T., Livesley, S. J., Duff, T. J., & Arndt, S. K. (2015). Changes in soil moisture drive soil methane uptake along a fire regeneration chronosequence in a eucalypt forest landscape. *Global Change Biology*, 21(11), 4250–4264. <https://doi.org/10.1111/gcb.13003>
- Fick, S. E., & Hijmans, R. J. (2017). WorldClim 2: New 1-km spatial resolution climate surfaces for global land areas. *International Journal of Climatology*, 37(12), 4302–4315. <https://doi.org/10.1002/joc.5086>
- Friedl, M., & Sulla-Menasse, D. (2022). MODIS/terra+Aqua land cover type yearly L3 global 500m SIN grid V061 [Dataset]. <https://doi.org/10.5067/MODIS/MCD12Q1.061>
- Gauci, V., Pangala, S. R., Shenkin, A., Barba, J., Bastviken, D., Figueiredo, V., et al. (2024). Global atmospheric methane uptake by upland tree woody surfaces. *Nature*, 631(8022), 796–800. <https://doi.org/10.1038/s41586-024-07592-w>
- Gilroy, J. J., Woodcock, P., Edwards, F. A., Wheeler, C., Baptiste, B. L. G., Medina Uribe, C. A., et al. (2014). Cheap carbon and biodiversity co-benefits from forest regeneration in a hotspot of endemism. *Nature Climate Change*, 4(6), 503–507. <https://doi.org/10.1038/nclimate2200>
- González, N. C., & Kröger, M. (2020). The potential of Amazon indigenous agroforestry practices and ontologies for rethinking global forest governance. *Forest Policy and Economics*, 118, 102257.
- Groffman, P. M., Butterbach-Bahl, K., Fulweiler, R. W., Gold, A. J., Morse, J. L., Stander, E. K., et al. (2009). Challenges to incorporating spatially and temporally explicit phenomena (hotspots and hot moments) in denitrification models. *Biogeochemistry*, 93(1), 49–77. <https://doi.org/10.1007/s10533-008-9277-5>
- Guariguata, M. R., & Ostertag, R. (2001). Neotropical secondary forest succession: Changes in structural and functional characteristics. *Forest Ecology and Management*, 148(1), 185–206. [https://doi.org/10.1016/S0378-1127\(00\)00535-1](https://doi.org/10.1016/S0378-1127(00)00535-1)
- Gurevitch, J., Koricheva, J., Nakagawa, S., & Stewart, G. (2018). Meta-analysis and the science of research synthesis. *Nature*, 555(7695), 175–182. <https://doi.org/10.1038/nature25753>
- Hatano, R., Toma, Y., Hamada, Y., Arai, H., Susilawati, H. L., & Inubushi, K. (2016). Methane and nitrous oxide emissions from tropical peat soil. In M. Osaki & N. Tsuji (Eds.), *Tropical peatland ecosystems* (pp. 339–351). Springer. https://doi.org/10.1007/978-4-431-55681-7_22
- Hayek, M. N., Harwatt, H., Ripple, W. J., & Mueller, N. D. (2020). The carbon opportunity cost of animal-sourced food production on land. *Nature Sustainability*, 4, 1–4. <https://doi.org/10.1038/s41893-020-00603-4>
- He, T., Ding, W., Cheng, X., Cai, Y., Zhang, Y., Xia, H., et al. (2024). Meta-analysis shows the impacts of ecological restoration on greenhouse gas emissions. *Nature Communications*, 15(1), 2668. <https://doi.org/10.1038/s41467-024-46991-5>
- Heinrich, V. H. A., Vancutsem, C., Dalagnol, R., Rosan, T. M., Fawcett, D., Silva-Junior, C. H. L., et al. (2023). The carbon sink of secondary and degraded humid tropical forests. *Nature*, 615(7952), 442. <https://doi.org/10.1038/s41586-022-05679-w>
- Hogan, J. A., Sharpe, J. M., Van Beusekom, A., Stankovich, S., Matta Carmona, S., Bithorn, J. E., et al. (2022). Solar radiation and soil moisture drive tropical forest understory responses to experimental and natural hurricanes. *Ecosphere*, 13(7), e4150. <https://doi.org/10.1002/ecs2.4150>
- Huddell, A. M., Galford, G. L., Tully, K. L., Crowley, C., Palm, C. A., Neill, C., et al. (2020). Meta-analysis on the potential for increasing nitrogen losses from intensifying tropical agriculture. *Global Change Biology*, 26(3), 1668–1680. <https://doi.org/10.1111/gcb.14951>
- IEA. (2023). *CO₂ emissions in 2022—Analysis and key findings*. A report by the International Energy Agency. Retrieved from <https://www.iea.org/reports/co2-emissions-in-2022>
- IPCC. (2022). Mitigation pathways compatible with 1.5°C in the context of sustainable development. In global warming of 1.5°C: IPCC special report on impacts of global warming of 1.5°C above pre-industrial levels in context of strengthening response to climate change. In *Sustainable development, and efforts to eradicate poverty* (pp. 93–174). Cambridge University Press. <https://doi.org/10.1017/9781009157940.004>
- IPCC. (2021). *Climate change 2021 – The physical science basis: Working group I contribution to the sixth assessment report of the inter-governmental panel on climate change* (1st ed.). Cambridge University Press. <https://doi.org/10.1017/9781009157896>
- Itoh, M., Kosugi, Y., Takanashi, S., Kanemitsu, S., Osaka, K., Hayashi, Y., et al. (2012). Effects of soil water status on the spatial variation of carbon dioxide, methane and nitrous oxide fluxes in tropical rain-forest soils in peninsular Malaysia. *Journal of Tropical Ecology*, 28(6), 557–570. <https://doi.org/10.1017/S0266467412000569>
- Jägermeyr, J., Müller, C., Ruane, A. C., Elliott, J., Balkovic, J., Castillo, O., et al. (2021). Climate impacts on global agriculture emerge earlier in new generation of climate and crop models. *Nature Food*, 2(11), 873–885. <https://doi.org/10.1038/s43016-021-00400-y>
- Jones, I. L., DeWalt, S. J., Lopez, O. R., Bunnefeld, L., Pattison, Z., & Dent, D. H. (2019). Above- and belowground carbon stocks are decoupled in secondary tropical forests and are positively related to forest age and soil nutrients respectively. *Science of The Total Environment*, 697, 133987. <https://doi.org/10.1016/j.scitotenv.2019.133987>
- Kharin, V. V., Zwiers, F. W., Zhang, X., & Wehner, M. (2013). Changes in temperature and precipitation extremes in the CMIP5 ensemble. *Climatic Change*, 119(2), 345–357. <https://doi.org/10.1007/s10584-013-0705-8>

- Kim, D.-G., Giltrap, D., & Hernandez-Ramirez, G. (2013). Background nitrous oxide emissions in agricultural and natural lands: A meta-analysis. *Plant and Soil*, 373(1–2), 17–30. <https://doi.org/10.1007/s11104-013-1762-5>
- King, M., Altdorff, D., Li, P., Galagedara, L., Holden, J., & Unc, A. (2018). Northward shift of the agricultural climate zone under 21st-century global climate change. *Scientific Reports*, 8(1), 7904. <https://doi.org/10.1038/s41598-018-26321-8>
- Knohl, A., Schulze, E.-D., Kolle, O., & Buchmann, N. (2003). Large carbon uptake by an unmanaged 250-year-old deciduous forest in central Germany. *Agricultural and Forest Meteorology*, 118(3), 151–167. [https://doi.org/10.1016/S0168-1923\(03\)00115-1](https://doi.org/10.1016/S0168-1923(03)00115-1)
- Koller, M. (2016). Robustlmm: An R package for robust estimation of linear mixed-effects models [Software]. *Journal of Statistical Software*, 75(6), 1–24. <https://doi.org/10.18637/jss.v075.i06>
- Koponen, H. T., & Martikainen, P. J. (2004). Soil water content and freezing temperature affect freeze–thaw related N₂O production in organic soil. *Nutrient Cycling in Agroecosystems*, 69(3), 213–219. <https://doi.org/10.1023/B:FRES.0000035172.37839.24>
- Lawrence, N. C., Tenesaca, C. G., VanLoocke, A., & Hall, S. J. (2021). Nitrous oxide emissions from agricultural soils challenge climate sustainability in the US corn belt. *Proceedings of the National Academy of Sciences*, 118(46), e2112108118. <https://doi.org/10.1073/pnas.2112108118>
- Li, Y., Chen, J., Drury, C. F., Liebig, M., Johnson, J. M. F., Wang, Z., et al. (2023). The role of conservation agriculture practices in mitigating N₂O emissions: A meta-analysis. *Agronomy for Sustainable Development*, 43(5), 63. <https://doi.org/10.1007/s13593-023-00911-x>
- Luyssaert, S., Schulze, E.-D., Börner, A., Knohl, A., Hessenmöller, D., Law, B. E., et al. (2008). Old-growth forests as global carbon sinks. *Nature*, 455(7210), 7210–7215. <https://doi.org/10.1038/nature07276>
- Martin-Benito, D., Pederson, N., Ferriz, M., & Gea-Izquierdo, G. (2021). Old forests and old carbon: A case study on the stand dynamics and longevity of aboveground carbon. *Science of The Total Environment*, 765, 142737. <https://doi.org/10.1016/j.scitotenv.2020.142737>
- Mason, K. E., Oakley, S., Street, L. E., Arróniz-Crespo, M., Jones, D. L., DeLuca, T. H., & Ostle, N. J. (2019). Boreal forest floor greenhouse gas emissions across a pleurozium schreberi-Dominated, wildfire-disturbed chronosequence. *Ecosystems*, 22(6), 1381–1392. <https://doi.org/10.1007/s10021-019-00344-2>
- McDaniel, M. D., Saha, D., Dumont, M. G., Hernández, M., & Adams, M. A. (2019). The effect of land-use change on soil CH₄ and N₂O fluxes: A global meta-analysis. *Ecosystems*, 22(6), 1424–1443. <https://doi.org/10.1007/s10021-019-00347-z>
- McDowell, N. G., Sapes, G., Pivovarov, A., Adams, H. D., Allen, C. D., Anderegg, W. R. L., et al. (2022). Mechanisms of woody-plant mortality under rising drought, CO₂ and vapour pressure deficit. *Nature Reviews Earth and Environment*, 3(5), 294–308. <https://doi.org/10.1038/s43017-022-00272-1>
- Melack, J. M., & Hess, L. L. (2023). Areal extent of vegetative cover: A challenge to regional upscaling of methane emissions. *Aquatic Botany*, 184, 103592. <https://doi.org/10.1016/j.aquabot.2022.103592>
- Myhre, G., Shindell, D., Bréon, F.-M., Collins, W., Fuglestedt, J., Huang, J., et al. (2013). 8 anthropogenic and natural radiative forcing. *Climate Change 2013: The Physical Science Basis. Contribution of Working Group I to the Fifth Assessment Report of the Intergovernmental Panel on Climate Change*.
- Nagano, H., Sugihara, S., Matsushima, M., Okitsu, S., Prikhodko, V. E., Manakhova, E., et al. (2012). Carbon and nitrogen contents and greenhouse gas fluxes of the Eurasian steppe soils with different land-use histories located in the Arkaim museum reserve of South Ural, Russia. *Soil Science & Plant Nutrition*, 58(2), 238–244. <https://doi.org/10.1080/00380768.2012.661354>
- Parsons, L. A. (2020). Implications of CMIP6 projected drying trends for 21st century Amazonian drought risk. *Earth's Future*, 8(10), e2020EF001608. <https://doi.org/10.1029/2020EF001608>
- Pugh, T. A. M., Arneth, A., Kautz, M., Poulter, B., & Smith, B. (2019). Important role of forest disturbances in the global biomass turnover and carbon sinks. *Nature Geoscience*, 12(9), 730–735. <https://doi.org/10.1038/s41561-019-0427-2>
- Raczka, N. C., Ho, Q. Y., Srinivasan, V., Lee, M. Y., Ko, C.-W., Königer, M., et al. (2023). Greater soil carbon losses from secondary than old-growth tropical forests. *Frontiers in Forests and Global Change*, 6, 1135270. <https://doi.org/10.3389/ffgc.2023.1135270>
- Ramankutty, N., Evan, A. T., Monfreda, C., & Foley, J. A. (2010). Global agricultural lands: Pastures, 2000 [Dataset]. <https://doi.org/10.7927/H47H1GGR>
- R Core Team. (2024). R: A language and environment for statistical computing [Software]. R Foundation for Statistical Computing. Retrieved from <https://www.R-project.org/>
- Robinson, N., Drever, R., Gibbs, D., Lister, K., Esquivel-Muelbert, A., Heinrich, V., et al. (2024). Protect young secondary forests for optimum carbon removal. *Research Square*. <https://doi.org/10.21203/rs.3.rs-4659226/v1>
- Saunio, M., Stavert, A. R., Poulter, B., Bousquet, P., Canadell, J. G., Jackson, R. B., et al. (2020). The global methane budget 2000–2017. *Earth System Science Data*, 12(3), 1561–1623. <https://doi.org/10.5194/essd-12-1561-2020>
- Schwartz, N. B., Aide, T. M., Graesser, J., Grau, H. R., & Uriarte, M. (2020). Reversals of reforestation across Latin America limit climate mitigation potential of tropical forests. *Frontiers in Forests and Global Change*, 3, 85. <https://doi.org/10.3389/ffgc.2020.00085>
- Sinha, V., Williams, J., Crutzen, P. J., & Lelieveld, J. (2007). Methane emissions from boreal and tropical forest ecosystems derived from in-situ measurements. *Atmospheric Chemistry and Physics Discussions*, 7(5), 14011–14039. <https://doi.org/10.5194/acpd-7-14011-2007>
- Solazzo, E., Crippa, M., Guizzardi, D., Muntean, M., Choulga, M., & Janssens-Maenhout, G. (2021). Uncertainties in the emissions database for global atmospheric research (EDGAR) emission inventory of greenhouse gases. *Atmospheric Chemistry and Physics*, 21(7), 5655–5683. <https://doi.org/10.5194/acp-21-5655-2021>
- Sze, J. S., Childs, D. Z., Carrasco, L. R., & Edwards, D. P. (2022). Indigenous lands in protected areas have high forest integrity across the tropics. *Current Biology*, 32(22), 4949–4956. <https://doi.org/10.1016/j.cub.2022.09.040>
- Taubert, F., Fischer, R., Groeneveld, J., Lehmann, S., Müller, M. S., Rödig, E., et al. (2018). Global patterns of tropical forest fragmentation. *Nature*, 554(7693), 519–522. <https://doi.org/10.1038/nature25508>
- Teixeira, R. S. da Fialho, R. C., Costa, D. C., de Sousa, R. N., Santos, R. S., Teixeira, A. P. M., et al. (2020). Land-use change with pasture and short rotation eucalypts impacts the soil C emissions and organic C stocks in the Cerrado biome. *Land Degradation and Development*, 31(7), 909–923. <https://doi.org/10.1002/ldr.3480>
- Terrer, C., Phillips, R. P., Hungate, B. A., Rosende, J., Pett-Ridge, J., Craig, M. E., et al. (2021). A trade-off between plant and soil carbon storage under elevated CO₂. *Nature*, 591(7851), 599–603. <https://doi.org/10.1038/s41586-021-03306-8>
- Tian, H., Chen, G., Lu, C., Xu, X., Ren, W., Zhang, B., et al. (2015). Global methane and nitrous oxide emissions from terrestrial ecosystems due to multiple environmental changes. *Ecosystem Health and Sustainability*, 1(1), 1–20. <https://doi.org/10.1890/EHS14-0015.1>
- Tian, H., Pan, N., Thompson, R. L., Canadell, J. G., Suntharalingam, P., Regnier, P., et al. (2023). Global nitrous oxide budget 1980–2020 [Preprint]. *ESSD – Global/Biogeosciences and biodiversity*. <https://doi.org/10.5194/essd-2023-401>
- Tian, H., Xu, R., Canadell, J. G., Thompson, R. L., Winiwarter, W., Suntharalingam, P., et al. (2020). A comprehensive quantification of global nitrous oxide sources and sinks. *Nature*, 586(7828), 248–256. <https://doi.org/10.1038/s41586-020-2780-0>

- Townsend, J., Moola, F., & Craig, M.-K. (2020). Indigenous Peoples are critical to the success of nature-based solutions to climate change. *FACETS*, 5(1), 551–556. <https://doi.org/10.1139/facets-2019-0058>
- UN FAO. (2012). Harmonized world soil database v1.2 [Dataset]. Retrieved from <https://data.apps.fao.org/catalog/dataset/harmonized-world-soil-database>
- Usuga, J. C. L., Toro, J. A. R., Alzate, M. V. R., & de Jesús Lema Tapias, Á. (2010). Estimation of biomass and carbon stocks in plants, soil and forest floor in different tropical forests. *Forest Ecology and Management*, 260(10), 1906–1913. <https://doi.org/10.1016/j.foreco.2010.08.040>
- Vasconcelos, S. S., Zarin, D. J., Capanu, M., Littell, R., Davidson, E. A., Ishida, F. Y., et al. (2004). Moisture and substrate availability constrain soil trace gas fluxes in an eastern Amazonian regrowth forest. *Global Biogeochemical Cycles*, 18(2). <https://doi.org/10.1029/2003GB002210>
- Verchot, L. V., Davidson, E. A., Cattaneo, J. H., & Ackerman, I. L. (2000). Land-use change and biogeochemical controls of methane fluxes in soils of Eastern Amazonia. *Ecosystems*, 3(1), 41–56. <https://doi.org/10.1007/s100210000009>
- Wang, X., Gao, S., Chen, J., Yao, Z., & Zhang, X. (2022). Reducing soil CO₂, CH₄ and N₂O emissions through management of harvest residues in Chinese fir plantation. *Forest Ecology and Management*, 511, 120140. <https://doi.org/10.1016/j.foreco.2022.120140>
- Wang, X., Hu, H.-B., Zheng, X., Deng, W.-B., Chen, J.-Y., Zhang, S., & Cheng, C. (2022). Will climate warming of terrestrial ecosystem contribute to increase soil greenhouse gas fluxes in plot experiment? A global meta-analysis. *Science of The Total Environment*, 827, 154114. <https://doi.org/10.1016/j.scitotenv.2022.154114>
- Weber, J., King, J., Abraham, N. L., Grosvenor, D., Smith, C. J., Shin, Y. M., et al. (2024). Chemistry-albedo feedbacks offset up to a third of forestation's CO₂ removal benefits. *Science*, 383(6685), 860–864. <https://doi.org/10.1126/science.adg6196>
- Wickham, H., Chang, W., Henry, L., Pedersen, T. L., Takahashi, K., Wilke, C., et al. (2025). ggplot2: Create elegant data visualisations using the grammar of graphics (version 3.5.2) [Software]. Retrieved from <https://cran.r-project.org/web/packages/ggplot2/index.html>
- Yavitt, J. B., Lang, G. E., & Sextone, A. J. (1990). Methane fluxes in wetland and forest soils, beaver ponds, and low-order streams of a temperate forest ecosystem. *Journal of Geophysical Research*, 95(D13), 22463–22474. <https://doi.org/10.1029/JD095iD13p22463>
- Yu, K., Smith, W. K., Trugman, A. T., Condit, R., Hubbell, S. P., Sardans, J., et al. (2019). Pervasive decreases in living vegetation carbon turnover time across forest climate zones. *Proceedings of the National Academy of Sciences*, 116(49), 24662–24667. <https://doi.org/10.1073/pnas.1821387116>
- Yvon-Durocher, G., Allen, A. P., Bastviken, D., Conrad, R., Gudas, C., St-Pierre, A., et al. (2014). Methane fluxes show consistent temperature dependence across microbial to ecosystem scales. *Nature*, 507(7493), 488–491. <https://doi.org/10.1038/nature13164>
- Zhang, H., Tang, C., Berninger, F., Bai, S., Wang, H., & Wang, Y. (2022). Intensive forest harvest increases N₂O emission from soil: A meta-analysis. *Soil Biology and Biochemistry*, 172, 108712. <https://doi.org/10.1016/j.soilbio.2022.108712>
- Zhao, J.-F., Peng, S.-S., Chen, M.-P., Wang, G.-Z., Cui, Y.-B., Liao, L.-G., et al. (2019). Tropical forest soils serve as substantial and persistent methane sinks. *Scientific Reports*, 9(1), 16799. <https://doi.org/10.1038/s41598-019-51515-z>
- Zheng, Y., Jin, Y., Ma, R., Kong, D., Zhu-Barker, X., Horwath, W. R., et al. (2020). Drought shrinks terrestrial upland resilience to climate change. *Global Ecology and Biogeography*, 29(10), 1840–1851. <https://doi.org/10.1111/geb.13160>
- Zhou, Y., Meng, D., Osborne, B., Fan, Y., & Zou, J. (2022). The impact of modifications in forest litter inputs on soil N₂O fluxes: A meta-analysis. *Atmosphere*, 13(742), 742. <https://doi.org/10.3390/atmos13050742>